The Journal of Neuroscience, May 1994, 14(5): 3122–3138

Morphologic and Biochemical Analysis of the Intracellular Trafficking of the Alzheimer β/A4 Amyloid Precursor Protein

Gregg L. Caporaso,[1] Kohji Takei,[2,3] Samuel E. Gandy,[1,4] Michela Matteoli,[3] Olaf Mundigl,[3] Paul Greengard,[1] and Pietro De Camilli[2,3]

[1]Laboratory of Molecular and Cellular Neuroscience, The Rockefeller University, New York, New York 10021, [2]Howard Hughes Medical Institute and [3]Department of Cell Biology, Yale University School of Medicine, Boyer Center for Molecular Medicine, New Haven, Connecticut 06536, and [4]Department of Neurology and Neuroscience, The New York Hospital–Cornell Medical Center, New York, New York 10021

Abnormal metabolic processing of the β/A4 amyloid precursor protein (APP) has been implicated in the pathogenesis of Alzheimer disease. Several aspects of normal APP processing have been elucidated, but the precise cellular trafficking of APP remains unclear. To investigate APP trafficking pathways further, we have examined the subcellular distribution of APP in rat brain tissue and a variety of cultured cell types, and correlated this distribution with the biochemical processing of APP.

In immunofluorescence microscopy of rat brain sections, APP immunoreactivity was concentrated in the Golgi complex and in proximal axon segments. In addition, a lower level of punctate fluorescence was visible throughout the neuropil. By immunoelectron microscopy of rat brain tissue fragments, APP was found associated with Golgi elements and with medium-sized, invaginated vesicles in both axons and dendrites. Prominent localization of APP to the Golgi complex was also found in primary cultures of rat hippocampal neurons and in non-neuronal cell lines.

When cultured cells were treated with brefeldin A (BFA), APP immunoreactivity changed from a Golgi-like to an endoplasmic reticulum-like distribution. No APP was detected in the BFA-induced reticulum identified by the transferrin receptor, indicating that concentration of APP in the Golgi does not reflect recycling between the *trans*-Golgi network and early endosomal system. In immunoblots of BFA-treated cells, there was an accumulation of full-length APP and inhibition of APP secretory processing. Treatment with phorbol ester resulted in a marked elevation of APP secretion, but no obvious redistribution of APP immunoreactivity was apparent at the light microscope level. The lysosomotropic drug chloroquine induced accumulation of APP in cell lysates, as seen by immunoblotting. Immunofluorescence microscopy of chloroquine-treated cells demonstrated a colocalization of APP with the lysosomal marker lgp120, whereas no colocalization was seen in untreated cells. Taken together, these results support a scheme in which APP is concentrated in the Golgi complex as it travels through the central vacuolar system en route to the plasma membrane for secretion of its amino-terminal domain and/or to lysosomes for degradation.

[Key words: Golgi complex, synaptic vesicles, brefeldin A, chloroquine, lysosomes, phorbol ester]

The extracellular deposition of β/A4 amyloid peptide in brain cortical parenchyma and cerebromeningeal blood vessels is a pathological hallmark of Alzheimer disease (Glenner and Wong, 1984; Tomlinson and Corsellis, 1984; Masters et al., 1985). The β/A4 peptide arises from proteolytic cleavage of the amyloid precursor protein (APP), a transmembrane glycoprotein that exists as multiple isoforms resulting from alternative splicing of a single transcript (Goldgaber et al., 1987; Kang et al., 1987; Robakis et al., 1987; Tanzi et al., 1987, 1988; Kitaguchi et al., 1988; Ponte et al., 1988). It is believed that abnormalities in the APP molecule or in its metabolism can give rise to Alzheimer disease. Several mutations in the APP gene have been identified in the kindred of patients suffering from early-onset, heritable forms of the disease (Chartier-Harlin et al., 1991; Goate et al., 1991; Murrell et al., 1991; Naruse et al., 1991; Mullan et al., 1992). Mutations in the APP gene are also apparently responsible for hereditary cerebral hemorrhage with amyloidosis (Dutch type), a rare inherited disorder in which deposition of β/A4 peptide in cerebral blood vessels produces fatal hemorrhages (Levy et al., 1990; Hendriks et al., 1992). Consequently, elucidation of the normal metabolic pathways of APP should provide a base for studying the processing abnormalities involved in the pathogenesis of these diseases.

Current evidence suggests the existence of multiple processing pathways for APP. One pool of APP molecules is cleaved within the β/A4 region, with the APP ectodomain secreted into cerebrospinal fluid and into the medium of cultured cells (Palmert et al., 1989; Weidemann et al., 1989; Oltersdorf et al., 1990). Since the proteolytic event that results in APP secretion occurs within the β/A4 domain of APP, it precludes a contribution of this population of molecules to amyloid deposits (Esch et al.,

Received June 28, 1993; revised Oct. 15, 1993; accepted Nov. 1, 1993.

We thank Drs. O. da Cruz e Silva and K. Iverfeldt for kindly providing COS cells, R. Cofiell for preparing rat brain sections, E. Griggs for providing photographic assistance, and Drs. M. Solimena and H. Stukenbrok for thoughtful discussions. We also thank Drs. K. Beyreuther, D. Bole, K. Buckley, I. Mellman, K. Moreman, I. Sandoval, J. Saraste, D. Selkoe, and I. Trowbridge for kindly providing antibodies. This research was supported by U.S. Public Health Service Medical Scientist Training Program Grant GM-07739 (G.L.C.), U.S. Public Health Service Grant AG-11508 and a Cornell Scholar Award in the Biomedical Sciences (S.E.G.), a long-term European Molecular Biology Organization fellowship (M.M.), U.S. Public Health Service Grants AG-09464 and AG-10491 (P.G.), a McKnight Endowment for the Neurosciences, and National Institute of Mental Health Grant MH 45191 (P.D.C.).

Correspondence should be addressed to Paul Greengard, Ph.D., Laboratory of Molecular and Cellular Neuroscience, The Rockefeller University, 1230 York Avenue, New York, NY 10021.

1990; Sisodia et al., 1990). The principal cellular site of APP secretory cleavage has not been determined, but recently it has been shown that at least some molecules may be cleaved at the cell surface (Sisodia, 1992). Although the kinetics of APP ectodomain secretion indicate that APP does not follow the standard regulated secretory pathway (Overly et al., 1991), APP secretion can be stimulated either by direct activation of protein kinase C with phorbol esters (Caporaso et al., 1992b; Gillespie et al., 1992; S. Sinha, personal communication) or by application of first messengers that act through protein kinase C (Buxbaum et al., 1992; Nitsch et al., 1992), suggesting a regulatory mechanism for this processing pathway. The mechanism by which protein kinase C modulates secretion of APP ectodomain has not been determined, although protein kinase C can phosphorylate APP *in vitro* (Gandy et al., 1988; Suzuki et al., 1992).

In most cell types that have been studied, the secretory pathway accounts for only a small fraction of total APP processing (Weidemann et al., 1989; Haass et al., 1991; Caporaso et al., 1992a; Knops et al., 1992). In rat neuroendocrine PC12 cells, the majority of APP molecules are proteolytically degraded in a chloroquine-sensitive intracellular compartment, presumably endosomes and/or lysosomes (Caporaso et al., 1992a). It has also been shown that full-length APP and APP degradative fragments are present in a lysosome-enriched subcellular fraction (Haass et al., 1992a), that potentially amyloidogenic APP fragments are probably processed in endosomes and lysosomes (Golde et al., 1992; Knops et al., 1992), and that APP immunoreactivity is present in neuronal structures identified as secondary lysosomes (Benowitz et al., 1989). Furthermore, full-length APP and the carboxyl-terminal APP fragment resulting from secretory cleavage are enriched in clathrin-coated vesicles, suggesting that these protein species are targeted to the endosomal system after endocytosis from the plasma membrane or directly from the *trans*-Golgi network (TGN) (Nordstedt et al., 1993). It was demonstrated recently that intact β/A4 peptide is released from cultured cells and is present in plasma and cerebrospinal fluid (Haass et al., 1992b; Seubert et al., 1992), and that production of secreted β/A4 might occur in the endosomal/lysosomal system (Shoji et al., 1992), additionally stressing the importance of this compartment in APP metabolism.

In the present study, the subcellular distribution of APP was examined in a variety of cell types in an attempt to elucidate APP trafficking further. Employing markers specific for individual cellular compartments and pharmacological agents known to affect organelle function or signal transduction, we correlate the localization of APP with the biochemical processing of the molecule.

Materials and Methods

Antibodies. Preparation of affinity-purified rabbit anti–carboxyl-terminal APP antibody (369A) has been described previously, and this antibody identifies immature and mature holomolecules of all APP isoforms as well as carboxyl-terminal APP fragments (Buxbaum et al., 1990). [It is possible that antibody 369A may, under some circumstances, cross-react with other proteins in the APP family (e.g., APLP1, Wasco et al., 1992, or APLP2, Wasco et al., 1993). Experiments designed to clarify this issue are underway.] Other antibodies were generous gifts, as follows: a monoclonal antibody against the amino terminus of APP (22C11; Dr. Konrad Beyreuther, University of Heidelberg, Heidelberg, Germany), polyclonal rabbit serum raised against the carboxyl terminus of APP (C7; Dr. Dennis Selkoe, Harvard Medical School, Boston, MA), a monoclonal antibody that recognizes an integral membrane protein of the *trans*-Golgi and TGN (GIMP$_t$; Dr. Ignacio Sandoval, Universidad Autónoma de Madrid, Cantoblanco, Madrid, Spain), a monoclonal antibody against the synaptic vesicle protein SV2 (Dr. Kathleen Buckley, Harvard Medical School, Boston, MA), a rabbit polyclonal antibody against mannosidase II (Dr. Kelley Moreman, Massachusetts Institute of Technology, Cambridge, MA), a rabbit polyclonal antibody against the intermediate compartment protein p58 (Dr. Jaakko Saraste, Ludwig Institute for Cancer Research, Stockholm, Sweden), a monoclonal antibody against the cytoplasmic domain of human transferrin receptor (Tf-R) (Dr. Ian Trowbridge, Salk Institute, San Diego, CA), a monoclonal antibody that recognizes the endoplasmic reticulum (ER) marker BiP (Dr. David Bole, University of Michigan, Ann Arbor, MI), and a monoclonal antibody against the lysosomal marker lgp120 (Dr. Ira Mellman, Yale University School of Medicine, New Haven, CT).

FITC-conjugated goat anti-mouse antibody was obtained from Sigma Chemical Co. (St. Louis, MO), and rhodamine-conjugated goat anti-rabbit antibody was obtained from Boehringer Mannheim Biochemicals (Indianapolis, IN). FITC-conjugated wheat germ agglutinin (WGA) was obtained from Vector Laboratories, Inc. (Burlingame, CA). FITC-conjugated lentil lectin was obtained from E-Y Laboratories (San Mateo, CA). Protein A–gold particles were prepared according to the method of Slot and Geuze (1985). Donkey anti-rabbit and sheep anti-mouse horseradish peroxidase–coupled secondary antibodies were purchased from Amersham Corp. (Arlington Heights, IL).

Cell cultures. Primary cultures of rat hippocampal neurons were prepared from 18-d-old fetal rats as described (Banker and Cowan, 1977; Bartlett and Banker, 1984). Cells were grown for 4 d on poly-L-lysine–treated glass coverslips in minimum essential medium without serum, containing 1% HL1 supplement (Ventrex, Portland, ME), 2 mM glutamine, and 1 mg/ml BSA.

Chinese hamster ovary (CHO) cells were grown in Dulbecco's modified Eagle's medium (DMEM) containing 10% heat-inactivated FBS, 34 μg/ml proline, 100 U/ml penicillin, and 100 μg/ml streptomycin. African green monkey kidney (COS) cells were grown in DMEM containing 10% heat-inactivated FBS, 20 mM HEPES (pH 7.4), and 1× antibiotic/antimycotic solution (GIBCO–Bethesda Research Labs, Gaithersburg, MD). Undifferentiated rat pheochromocytoma (PC12) cells were grown in DMEM containing 10% heat-inactivated FBS, 5% heat-inactivated horse serum, and 1× antibiotic/antimycotic solution. Rat insulinoma (RINm5F) cells (Gazdar et al., 1980) were grown in RPMI 1640 medium containing 10% fetal calf serum. Mouse insulinoma (βTC3) cells (Efrat et al., 1988) were grown in Click medium (Irvine Scientific, Santa Ana, CA) containing 5% fetal calf serum. Primary cultures and all cell lines were grown in 5% CO_2 at 37°C.

Drug treatments. Brefeldin A (BFA) was obtained from Epicentre Technologies (Madison, WI) and was stored at −20°C as a 1000× stock solution of 10 mg/ml in methanol. Phorbol 12,13-dibutyrate (PDBu) was obtained from LC Services (Woburn, MA) and was stored at −20°C as a 1000× stock solution of 1 mM in 50% dimethyl sulfoxide. Chloroquine was obtained from Sigma Chemical Co. and was stored at 4°C as a 1000× stock solution of 50 mM. Cells were incubated for the indicated times in medium containing drug, and then washed prior to fixation for immunocytochemistry or prior to lysis for immunoblot analysis.

Immunofluorescence labeling. Cells were grown for 2–3 d on poly-L-ornithine–coated glass coverslips. Following incubation in medium alone or in medium containing drugs, cells were washed once with 120 mM phosphate buffer (pH 7.4) and then fixed for 30 min at 37°C with 4% formaldehyde (freshly prepared from paraformaldehyde), 4% sucrose in 120 mM phosphate buffer. All subsequent steps were performed at room temperature. After a wash with high-salt PBS (500 mM NaCl, 20 mM phosphate buffer), cells were incubated for 30 min with "goat serum dilution buffer" (GSDB; 0.45 M NaCl, 20 mM phosphate buffer, 0.3% Triton X-100, 17% goat serum) in order to permeabilize membranes and block nonspecific secondary antibody binding sites. Cells were next incubated for 2–3 hr with primary antibodies prepared in GSDB. Following washes with high-salt PBS, cells were incubated for 30–90 min with fluorescent secondary antibodies prepared in GSDB. Cells were washed with high-salt PBS and then briefly with 5 mM phosphate buffer before mounting the coverslips onto glass slides using freshly prepared mounting solution [70% glycerol, 1 mg/ml *p*-phenylenediamine (Sigma Chemical Co.), 150 mM NaCl, 10 mM phosphate buffer]. Slides were viewed with a Zeiss Axiophot microscope equipped with epifluorescence optics and photographed with Kodak TMAX-100 film.

Brains of adult Sprague–Dawley rats (150–200 gm) were fixed by perfusion with 4% paraformaldehyde in 120 mM phosphate buffer and 7 μm sections were prepared (De Camilli et al., 1983a). Brain sections were labeled for immunofluorescence microscopy essentially as described above.

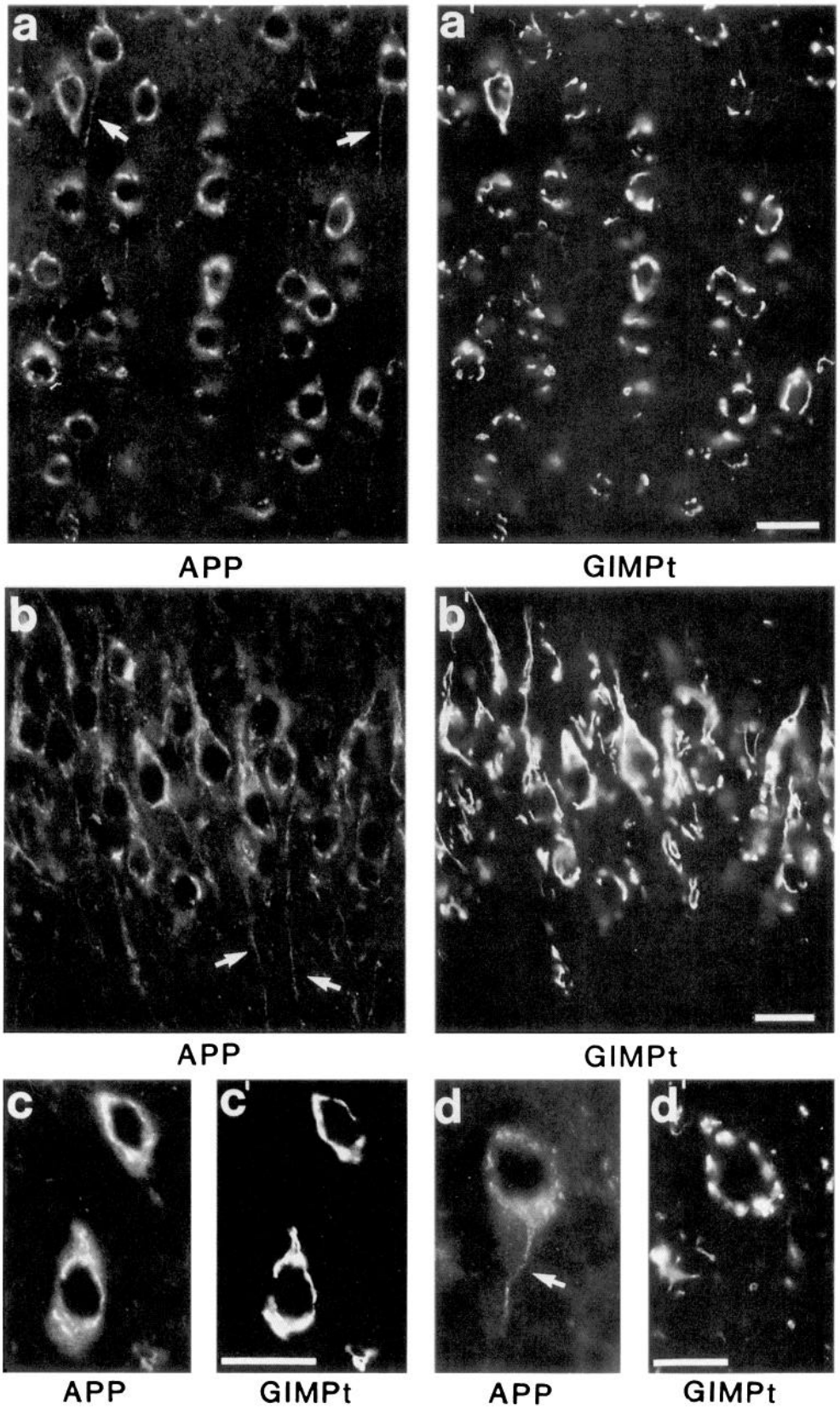

Figure 1. Comparison of the subcellular localization of APP and GIMP$_t$ in rat brain by immunofluorescence microscopy. Rat brain sections were double labeled for APP (antibody 369A) (*a–d'*) and GIMP$_t$ (*a'–d'*). The following populations of cells are shown: *a, a'*, cortical forebrain pyramidal cells; *b, b'*, hippocampal pyramidal cells; *c, c'*, brainstem neurons; and *d, d'*, cerebellar Purkinje cells. APP immunoreactivity in the proximal segment of axons is indicated (*arrows*). Scale Bars, 20 μm.

Immunoelectron microscopy. Preparation of agarose-embedded rat brain tissue fragments and immunoelectron microscopy were performed as described previously (De Camilli et al., 1983b; Takei et al., 1992).

Immunoblot analysis. Cells were grown for 2–3 d on 6 cm culture dishes. Following drug treatment, the medium was removed, the cells were washed with 120 mM phosphate buffer or Hank's balanced saline solution and scraped from the dishes in 400–600 μl of 1% SDS, and the lysates were boiled and sonicated. Following centrifugation at 14,000 × *g* for 10 min, supernatants were assayed for total protein using the BCA system (Pierce, Rockford, IL). Aliquots of cell lysates containing

equal amounts of protein, or volumes of medium normalized for cell lysate protein, were diluted and boiled in sample buffer, separated on SDS-polyacrylamide gels by electrophoresis under reducing conditions (Laemmli, 1970), and transferred to nitrocellulose membranes (Towbin et al., 1979). The procedure for immunoblotting has been described elsewhere (Nordstedt et al., 1993). Immunoreactivity was visualized with the enhanced chemiluminescence system (Amersham Corp.) according to the manufacturer's instructions, and blots were exposed to x-ray film.

Pulse-chase labeling and immunoprecipitation. Experimental procedures for ^{35}S-methionine pulse labeling of CHO cells and immunoprecipitation using antibody 369A were essentially as described previously (Caporaso et al., 1992a). When APP maturation was examined, immunoprecipitates were treated with endoglycosidase H (endo H) (Boehringer Mannheim Biochemicals) for 16 hr or with neuraminidase (Boehringer Mannheim Biochemicals) for 2 hr at 37°C as described (Teixidó and Massagué, 1988). Control samples were treated with enzyme buffer alone for 16 hr at 37°C. Incubations were stopped by the addition of 5× gel sample buffer and boiling.

Results

APP is concentrated in the Golgi complex of neurons and in vesicular structures of dendrites and axons

To examine the subcellular localization of APP, rat brains were fixed by perfusion with formaldehyde and cryosectioned, and 7 μm slices were examined by immunofluorescence microscopy (De Camilli et al., 1983a) with an antibody against the carboxyl terminus of APP (369A; Buxbaum et al., 1990). In the brain regions studied—forebrain, hippocampus, brainstem, and cerebellum—most neurons were intensely APP immunoreactive (Fig. 1). Some APP immunoreactivity was also detected in a variety of supporting cells, including glial cells. APP was observed predominantly in perinuclear structures in all cell types. In neurons, this intense immunoreactivity extended into the proximal portions of cell processes.

This distribution was suggestive of a concentration of APP in the region of the neuronal Golgi complex (De Camilli et al., 1986). Brain sections were therefore double labeled with an antibody directed against GIMP$_1$, an integral membrane protein localized to the *trans*-Golgi and TGN (Yuan et al., 1987). Cellular areas of the greatest APP immunoreactivity coincided with GIMP$_1$-immunoreactive areas in perikarya and dendrites (Fig. 1). In addition, high levels of APP staining were found in the proximal portion of axons, which do not contain elements of the Golgi complex (De Camilli et al., 1986) and which were accordingly negative for GIMP$_1$ immunoreactivity (Fig. 1*a,a',b,b'*). A high-power view of a cerebellar Purkinje cell with its initial axonal segment is shown in Figure 1, *d* and *d'*. APP immunoreactivity extended along the axon into the granule cell layer (Fig. 1*d*). This staining became weaker with increasing distance from the perikaryon. Diffuse punctate APP immunofluorescence was present throughout the neuropil (compare the background immunofluorescence of Fig. 1, *a–d*, with that of *a'–d'*), but no accumulation of APP was seen at synapses.

A predominant localization of APP in the region of the Golgi complex was also observed in neurons in culture (Banker and Cowan, 1977; Bartlett and Banker, 1984) (Fig. 2*a*). In addition, in these cells a moderate to intense APP immunoreactivity was present as fine puncta in neuronal processes. APP was not concentrated at synaptic vesicles, however, as indicated by double labeling for the synaptic vesicle protein SV2 (Buckley and Kelly, 1985) (Fig. 2*b*).

To confirm the Golgi localization of APP and to examine the nature of the APP immunoreactivity seen in neuronal processes, fragments of brain tissue were obtained by coarse homogenization, embedded in agarose, immunogold labeled for APP, and finally Epon embedded (De Camilli et al., 1983b; Takei et al., 1992). In fragments of the Golgi complex, the presence of gold particles on cisternae was visible (Fig. 3*a*). This labeling of the Golgi complex was not seen in control preparations reacted with preimmune serum.

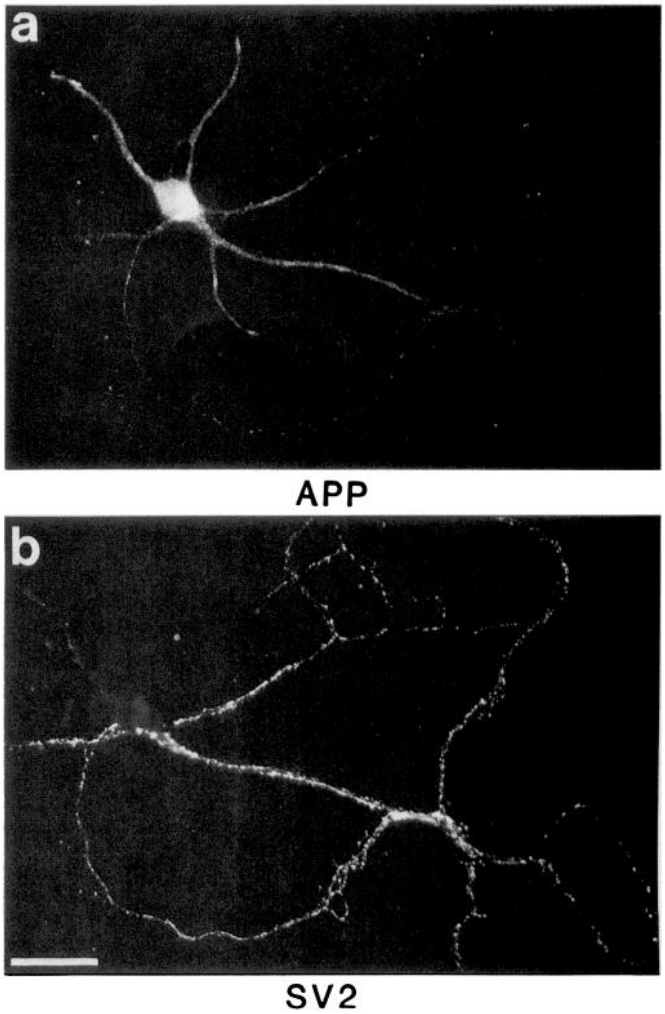

Figure 2. Localization of APP and SV2 in primary cultures of rat hippocampal neurons by immunofluorescence microscopy. Hippocampal neurons were grown in culture for 4 d before fixation and double labeled for APP (antibody 369A) (*a*) and SV2 (*b*). Scale bar, 20 μm.

In microscopic fields containing fragments of cell processes and synapses, APP immunoreactivity was found to be associated with medium-sized vesicles, many of which were characterized by outer and inner membranes, the latter appearing to arise by the invagination of the outer membrane (Fig. 3*b–f*). Gold particles were found at the cytoplasmic face of the outer membrane of these structures. The vesicles decorated with gold particles were seen both in myelinated (Fig. 3*b,c*) and in unmyelinated (Fig. 3*d*) axons as well as in pre- and postsynaptic compartments (Fig. 3*e,f*). No other dendritic or axonal structures were labeled, nor were the majority of synaptic vesicles (Fig. 3*e,f*).

Golgi localization of APP in cultured non-neuronal cells

Since we wished to determine the effects of experimental manipulations on the subcellular distribution of APP, several mam-

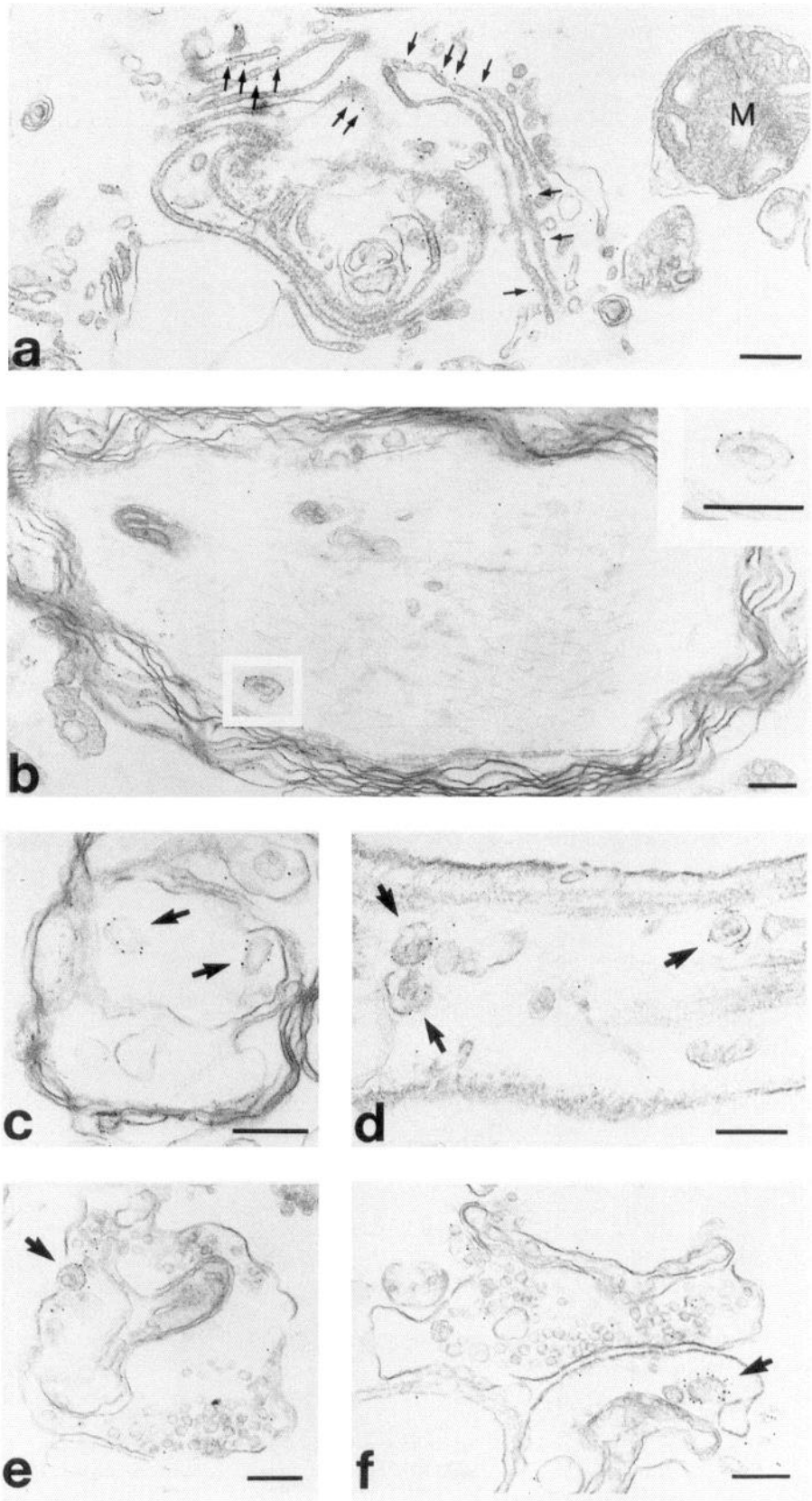

Figure 3. Localization of APP in rat brain tissue fragments by immunoelectron microscopy. Rat brain tissue fragments from forebrain (*a, b, d*) or from cerebellum plus brainstem (*c, e, f*) were embedded in agarose and probed with antibody 369A and colloidal gold-conjugated protein A prior to plastic embedding. APP immunoreactivity, as revealed by gold particle accumulation, is visible on Golgi membranes (*small arrows, a*) and on medium-sized vesicles (*large arrows* and *b, inset*) in cell processes (*b, c, d*), including myelinated (*b, c*) axons, and in pre- (*e*) and postsynaptic compartments (*f*). Some of these vesicles contain an internal membrane that appears to originate by an invagination of the outer membrane. A mitochondrion is indicated in *a* (*M*). Scale bars, 200 nm.

malian cell lines were examined to select a cell type appropriate for immunofluorescence microscopy of APP. Mouse insulinoma (βTC3), rat insulinoma (RINm5F), rat pheochromocytoma (PC12), African green monkey kidney (COS), and Chinese hamster ovary (CHO) cells all exhibited a predominant concentration of APP at a juxtanuclear location, with fine punctate staining seen in the cytoplasm (Fig. 4). The juxtanuclear staining coincided with the localization of the Golgi complex and pri-

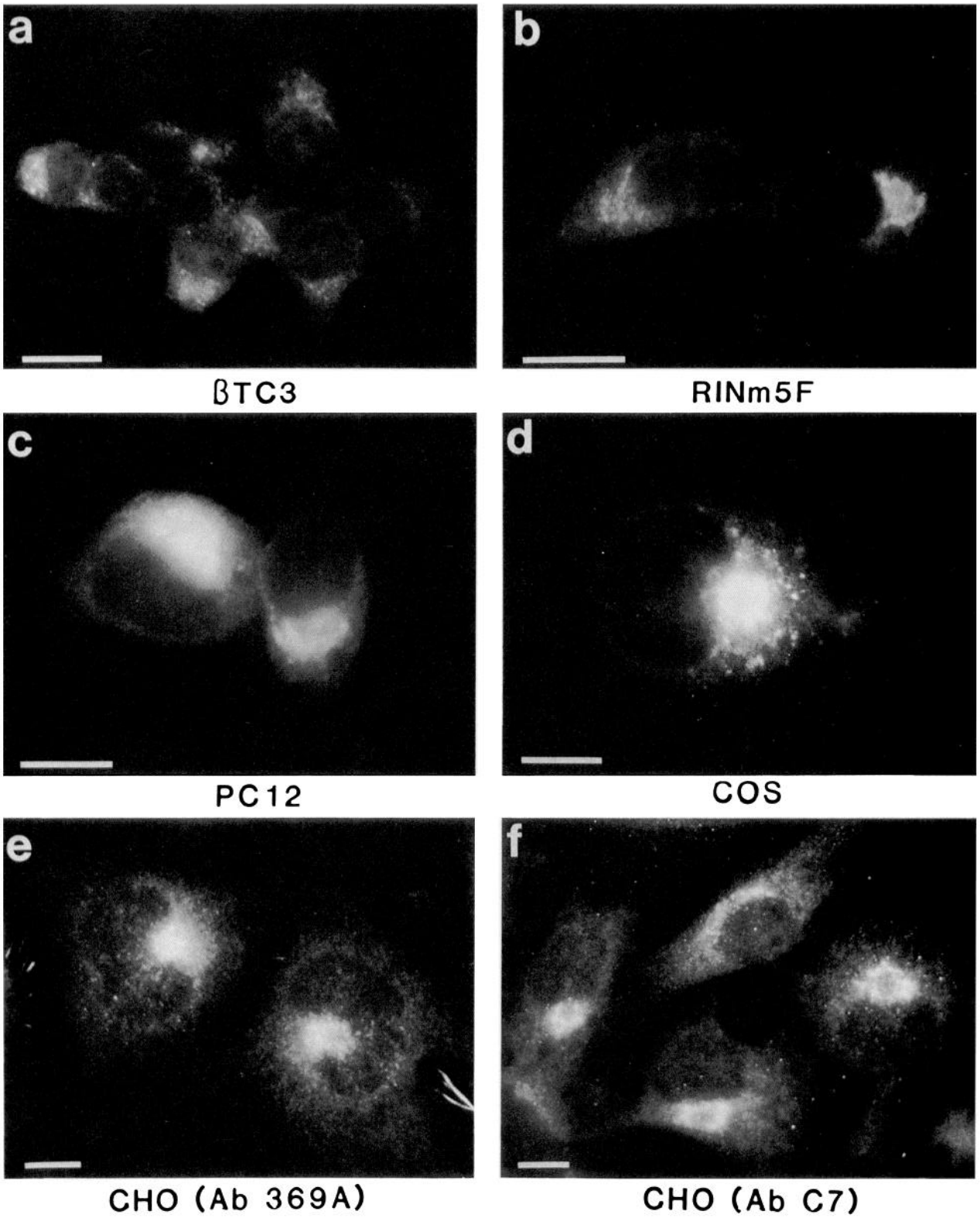

Figure 4. Immunofluorescence microscopy of various mammalian cell lines showing the juxtanuclear localization of APP. βTC3 (*a*), RINm5F (*b*), PC12 (*c*), and COS (*d*) cells were labeled with antibody 369A, and CHO cells were labeled with antibodies 369A (*e*) or C7 (*f*). Scale bars, 10 μm.

marily with that of the TGN (see below). Another carboxyl-terminal APP antibody, C7 (Podlisny et al., 1991), presented an identical pattern of APP immunoreactivity (Fig. 4*f*). This pattern was not seen with preimmune serum or when antibody 369A was preincubated with a synthetic peptide corresponding to the cytoplasmic domain of APP ($APP^{645-694}$; APP_{695} numbering system) (not shown).

On immunoblots of these cell types (Fig. 5), antibody 369A

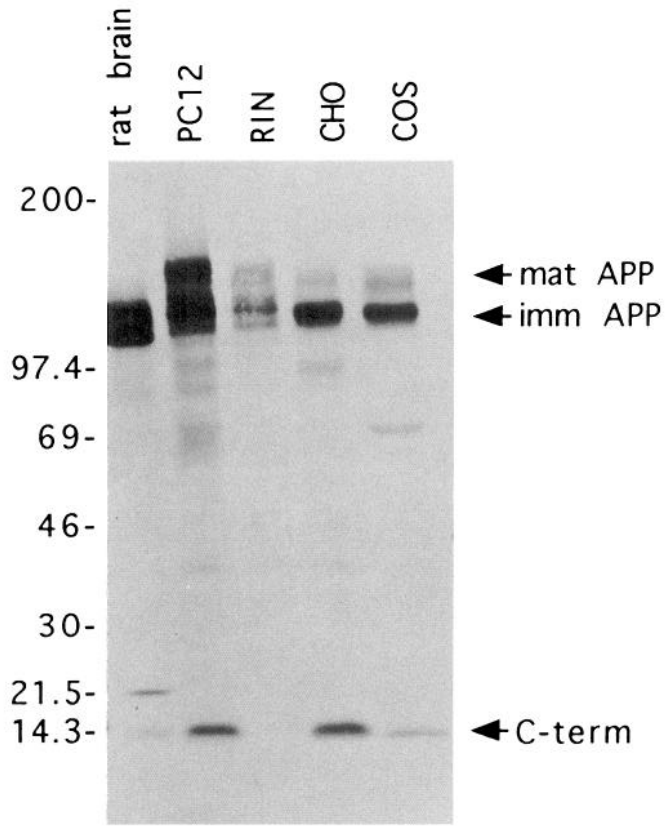

Figure 5. Immunoblot analysis of APP in rat brain and mammalian cell lines. Proteins (50 μg) from a rat cerebellar homogenate and from cell lysates of PC12, RINm5F, CHO, and COS cells were separated on a 4–15% continuous gradient SDS-polyacrylamide gel, and then transferred to nitrocellulose membrane and probed with antibody 369A. The identities of immature and mature full-length APP and the carboxyl-terminal APP fragment resulting from secretory processing are indicated for the cell lines. Relative molecular masses are in kilodaltons.

recognized proteins corresponding in apparent molecular mass to previously identified APP species (Weidemann et al., 1989; Buxbaum et al., 1990; Caporaso et al., 1992b). There were differences between cell types, though, in the relative intensities of specific APP bands. For example, PC12 cells contained abundant amounts of mature (completely glycosylated) full-length APP (Caporaso et al., 1992b), whereas both CHO and COS cells contained mostly APP species that comigrated with the protein bands corresponding to immature full-length APP in PC12 cells. Much lower levels of mature full-length APP were present in these cells. CHO and COS cells were also found to produce predominantly the 751/770 amino acid isoforms of APP, as indicated by an antibody specific for these species (Caporaso et al., 1992b) (not shown). CHO and COS cells also contained relatively high levels of an approximately 14 kDa APP-immunoreactive protein that comigrated with an immunoreactive band in PC12 cells, which was previously identified (Caporaso et al., 1992a) as the carboxyl-terminal fragment resulting from APP secretory cleavage (Esch et al., 1990; Sisodia et al., 1990). Because of the large size of CHO and COS cells, and their relative abundance of APP, these cells were selected for further microscopic study.

To confirm the Golgi localization of APP, several well-characterized markers of the Golgi complex were used (the antibody recognizing $GIMP_t$ did not react with CHO or COS cells). In CHO cells, APP was found to be concentrated in the region of the cell that stained most intensely for WGA, a lectin that binds with high affinity, although not selectively, to the Golgi complex (Virtanen et al., 1980; Tartakoff and Vassalli, 1983) (Fig. 6*a,a'*). The most intense APP immunoreactivity closely coincided with the distribution of lentil (*Lens culinaris*) lectin, which specifically labels glycoproteins of the Golgi complex (Ridgway et al., 1992) (Fig. 6*b,b'*), as shown by its colocalization with the Golgi-specific enzyme mannosidase II (Novikoff et al., 1983; Moreman and Touster, 1985) (Fig. 6*c,c'*). Similar results were obtained in COS cells (not shown).

The pattern of APP immunoreactivity in CHO cells was not suggestive of a localization to the *cis*-Golgi network, the transitional or intermediate compartment between the ER and the Golgi stacks. This was shown by staining CHO cells for APP and for the intermediate compartment and *cis*-Golgi marker p58 (Saraste et al., 1987). Although there was some overlap between the distributions of the two proteins, p58 immunoreactivity also extended away from the Golgi region (Fig. 7). APP staining, in contrast, appeared to be excluded from these extensions.

To evaluate the time course of APP transport through the Golgi complex, CHO cells were pulse labeled for 5 min with ^{35}S-methionine and then chased in the absence of labeled methionine (Fig. 8, top). The levels of immature APP remained unchanged for the first 10 min of chase, with no labeled mature APP being recovered. Mature APP was detected at 15 min, and the levels of mature APP peaked at 30 min, with a corresponding decrease in the levels of immature APP. By 60 min of chase, the levels of both immature and mature APP were substantially diminished.

The nature of the biochemical difference(s) between immature and mature APP was examined by treating the immunoprecipitates from pulse-labeled cells with endo H and neuraminidase, which cleave from proteins, high-mannose-type glycans, and sialic acid moieties, respectively (Fig. 8, bottom). When immunoprecipitates were incubated with endo H, there was a slight increase in the migration (~2 kDa) of the immature APP bands, with no change in the migration of mature APP. In contrast, neuraminidase treatment affected only mature APP, resulting in a shift of the mature APP species to a position comigrating with immature APP. These experiments indicate that immature APP is a high-mannose form of APP, characteristic of an ER and possibly *cis*-Golgi localization. The shift in migration of mature APP seems to be solely the result of addition of sialic acid, which is a *trans*-Golgi/TGN protein modification (Griffiths and Simons, 1986). These results are in close agreement with the posttranslational modifications demonstrated for APP in other cell types (Weidemann et al., 1989; Oltersdorf et al., 1990). Taken together with the results of the pulse-chase time course, it appears that approximately 15 min is the minimum time required for APP synthesis, transport through the ER and Golgi stacks, and arrival at the distal Golgi, where APP is sialylated.

BFA induces a redistribution of APP from a Golgi to an ER localization

To examine further the Golgi localization of APP, we used BFA, a fungal metabolite that induces disappearance of the Golgi complex and a relocation of its components into pre- and post-Golgi compartments (Pelham, 1991; Klausner et al., 1992). Treatment of cells with BFA results in a functional and spatial

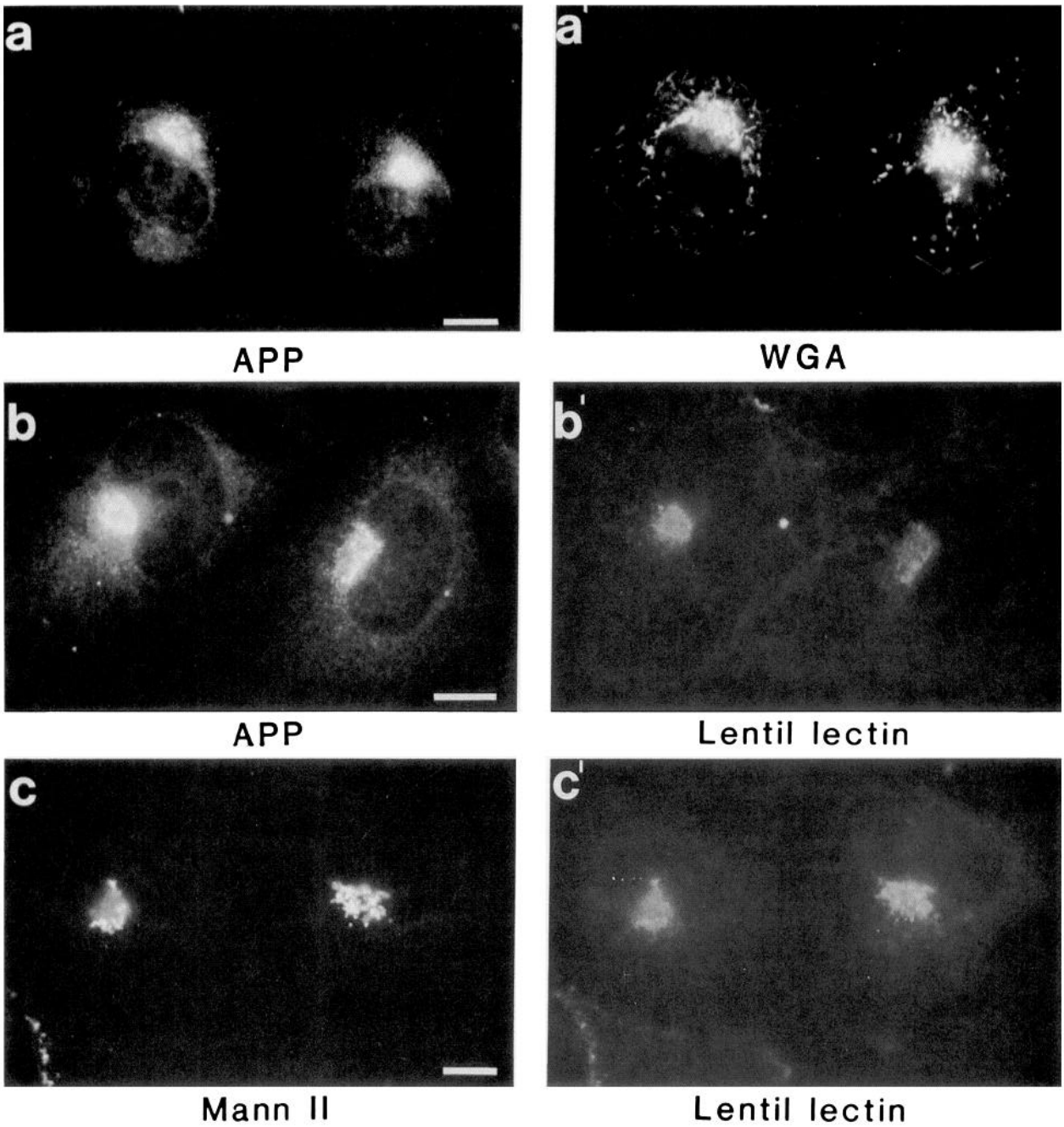

Figure 6. Comparison of the distributions of APP and several Golgi complex markers by fluorescence microscopy in CHO cells. Cells were double labeled for APP (antibody 369A; *a*) and WGA (*a'*), for APP (*b*) and lentil lectin (*b'*), or for mannosidase II (*c*) and lentil lectin (*c'*). Scale bars, 10 μm.

dissection of the *trans*-Golgi from the TGN (Chege and Pfeffer, 1990; Reaves and Banting, 1992). Specifically, BFA causes a resorption of *cis*-, middle-, and *trans*-Golgi proteins and membranes to the ER (Doms et al., 1989; Lippincott-Schwartz et al., 1989). At the same time, BFA has also been shown to produce fusion of the TGN and early endosomes into a tubular network (Lippincott-Schwartz et al., 1991; Wood et al., 1991).

We have previously demonstrated in PC12 cells that BFA interferes with normal posttranslational modification of APP and completely abolishes secretion and proteolytic turnover of APP (Caporaso et al., 1992a). Similar results were obtained in CHO cells treated with BFA and analyzed by immunoblotting (Fig. 9). In untreated cells, most detectable APP consisted of the immature full-length molecule, with mature full-length APP and the carboxyl-terminal APP fragment representing minor species. After 30 min of BFA treatment, the protein band corresponding to immature APP was slightly shifted to a higher molecular mass; by 2 hr of BFA treatment, APP immunoreactivity comprised a broad band spanning the positions of immature and mature APP (Fig. 9). At the peak effect of BFA treatment, the intensity of the full-length APP band was greater than that in control cells, suggesting an overall accumulation of APP inside the cells. In addition, the carboxyl-terminal APP fragment was scarcely visible, indicating that secretory cleavage

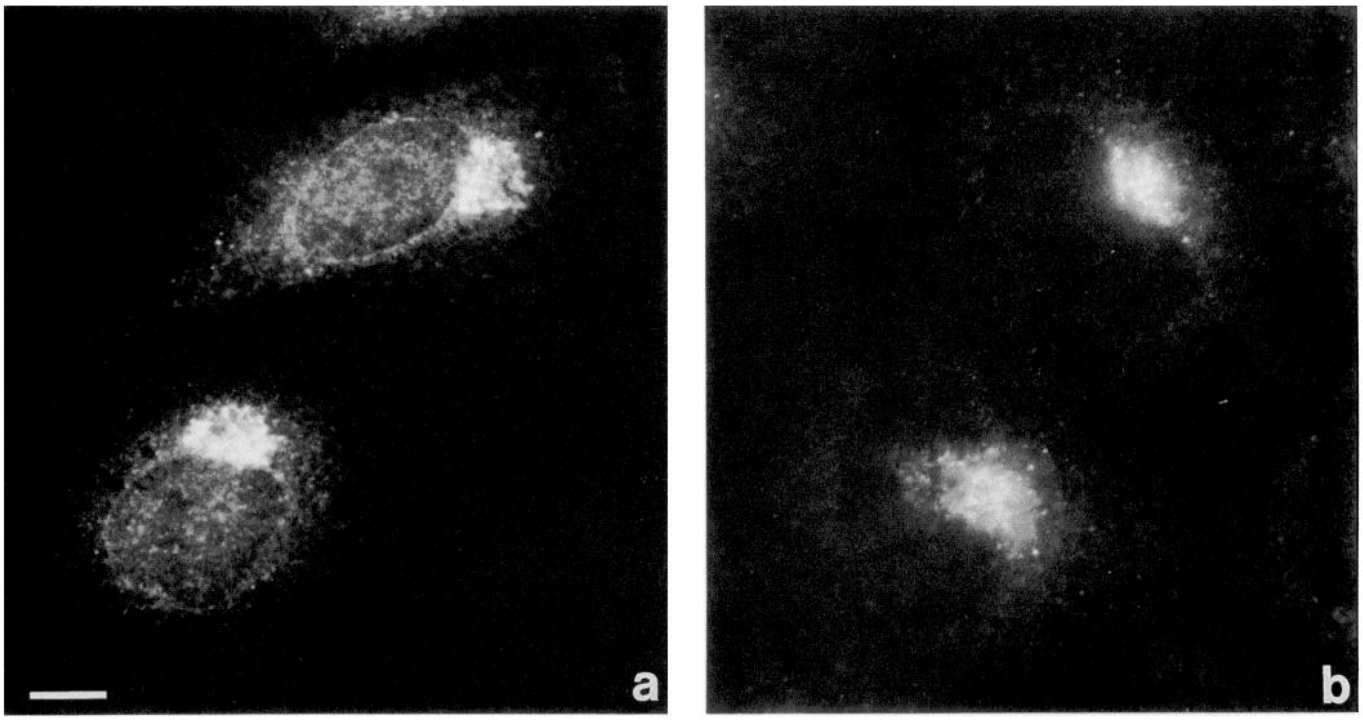

Figure 7. Comparison of the distributions of APP and p58 by immunofluorescence microscopy in CHO cells. Cells were labeled in parallel for APP (antibody 369A; *a*) and p58 (*b*). Scale bar, 10 μm.

had been inhibited. The effects of BFA on APP metabolism were reversible; 2 hr after removal of BFA, all APP species had returned to their pretreatment states (Fig. 9).

We next examined the effects of BFA on the subcellular localization of APP. Assuming that APP is not a resident Golgi protein (see Discussion), there are two plausible explanations for the intense APP immunoreactivity seen in the region of the Golgi complex. First, the abundance of APP in the Golgi complex might reflect its concentration in the distal Golgi as the protein travels through the central vacuolar system and is sorted in the TGN (Griffiths and Simons, 1986). In this case, upon BFA treatment one might expect a change in the distribution of APP immunoreactivity, resulting both from the rapid dispersal and clearance of APP molecules in the TGN to their post-Golgi destinations (e.g., constitutive secretory vesicles), and from the accumulation of newly synthesized APP in the ER–Golgi hybrid compartment (Doms et al., 1989; Lippincott-Schwartz et al., 1989; Chege and Pfeffer, 1990). Such a result would be consistent with the accumulation of full-length APP seen with the immunoblots of BFA-treated cells (Fig. 9). Alternatively, the pattern of APP staining might represent a population of molecules in the TGN that is involved in recycling among the TGN, early endosomes, and the plasma membrane. In this case, APP should be present in the tubular reticulum resulting from the BFA-induced fusion of these compartments (Lippincott-Schwartz et al., 1991; Wood et al., 1991).

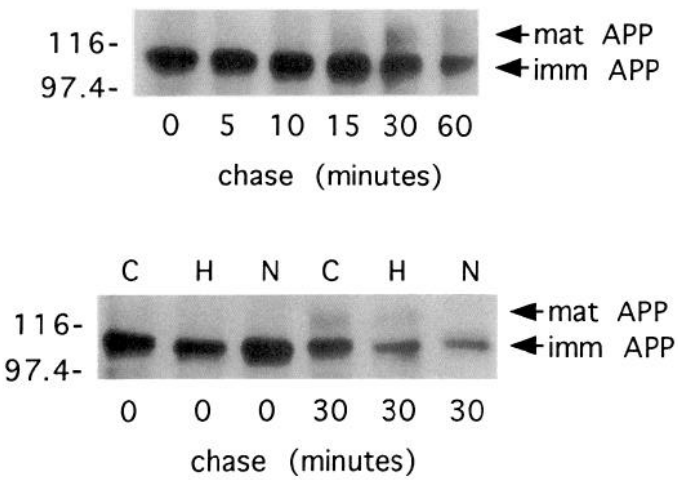

Figure 8. Pulse-chase analysis of APP maturation and processing in CHO cells. Cells were pulse labeled with ^{35}S-methionine for 5 min, and then chased in the presence of excess unlabeled methionine for 5, 10, 15, 30, or 60 min. APP species were immunoprecipitated with antibody 369A and separated on a 4–15% SDS-polyacrylamide gel, treated for fluography, and exposed to film. *Top,* Time course of full-length APP maturation and turnover. *Bottom,* Immunoprecipitates from 0 and 30 min chase intervals were mock treated (*C*), or incubated with endo H (*H*) or neuraminidase (*N*) prior to gel electrophoresis. The identities of immature and mature full-length APP are indicated. Relative molecular masses are in kilodaltons.

CHO cells were double labeled for APP and Tf-R, a protein known to recycle between the TGN and endosomes (Stoorvogel et al., 1988; Cameron et al., 1991), and which can be used as a marker of the BFA-induced reticulum formed from these two compartments (Lippincott-Schwartz et al., 1991). In untreated cells, both APP and Tf-R staining were most concentrated in the region of the Golgi complex, but intense punctate Tf-R immunoreactivity extended from the centrosomal region to the cell periphery (Fig. 10*a,a'*). Upon treatment with 10 μg/ml BFA for 30 min, a network of tubules emanating from the Golgi region was stained for Tf-R (Fig. 10*b'*) (Lippincott-Schwartz et al., 1991). In contrast, BFA treatment resulted in a more diffuse APP staining (Fig. 10*b*). There was no apparent colocalization

of APP with the tubular network identified by Tf-R. After 4 hr in the presence of BFA, cells exhibited a fine meshwork of APP immunostaining throughout the cytoplasm that resembled the structure of the ER (Fig. 10*c,d*) (see below).

Similar results were obtained in COS cells double labeled for APP and Tf-R before and after BFA treatment (Fig. 11*a,a',b,b'*). In these cells, the tubular network positive for Tf-R (Fig. 11*b'*) was not as well defined as that seen in CHO cells (Fig. 10*b'*).

Since the cellular distribution of APP after BFA treatment was suggestive of an ER localization, COS cells were double labeled for APP and BiP, an ER-resident protein (Bole et al., 1986). The distribution of BiP was the same in both untreated and BFA-treated cells, and consisted of a fine network of staining extending to the cell periphery (Fig. 11*c',d'*). When cells were treated with BFA, the immunolocalization of APP was very similar to that of BiP (Fig. 11*d,d'*), although some difference in fine details was observed.

Phorbol ester–stimulated APP secretion is not accompanied by an obvious redistribution of APP immunoreactivity

Activation of protein kinase C by phorbol esters has been shown previously to stimulate the proteolytic processing and secretion of APP in PC12, human embryonic kidney (293), and human mononuclear leukemia (K562) cells (Buxbaum et al., 1990; Caporaso et al., 1992b; Gillespie et al., 1992; Sinha, personal communication). To determine whether phorbol esters would stimulate APP secretion from CHO cells, cells were incubated with 1 μM PDBu and both the medium and cell lysates were analyzed by immunoblotting with an antibody directed against the amino terminus of APP (22C11; Weidemann et al., 1989) (Fig. 12). PDBu produced a severalfold increase in APP secretion that was apparent as early as 15 min following initiation of treatment and that continued for at least 2 hr (Fig. 12, bottom).

Concomitant with the increase in secretion, there was a decrease in levels of mature full-length APP observed between 15 min and 1 hr of PDBu treatment (Fig. 12, middle). [The increase in levels of mature APP seen at 2 hr might reflect the protein kinase C–mediated upregulation of APP gene expression (Goldgaber et al., 1989).] This suggests that the secreted form of APP may arise by proteolytic cleavage of mature full-length APP. Consistent with this model, PDBu had no detectable effects on the steady-state level of immature full-length APP (Fig. 12, top).

Despite the dramatic effects that phorbol ester produced on APP secretion, no changes were observed in the immunofluorescent pattern produced by any of several antibodies directed against the carboxyl terminus of APP in CHO cells after PDBu treatment (not shown).

APP accumulates in the lysosomes of chloroquine-treated cells

There is considerable evidence for a role of lysosomes in the processing of APP. In PC12 cells, the majority of mature full-length APP molecules are proteolytically degraded in a chloroquine-sensitive cellular compartment that is distinct from the site where APP secretory cleavage occurs (Caporaso et al., 1992a). It has also been shown that APP holomolecules and carboxyl-terminal fragments can be recovered from a subcellular fraction enriched in lysosomes (Haass et al., 1992a). In addition, clathrin-coated vesicles purified from PC12 cells are enriched in mature full-length APP and the carboxyl-terminal APP fragment resulting from secretory cleavage, indicating that these proteins are targeted to the endosomal system and, presumably, to lysosomes as their final destination (Nordstedt et al., 1993).

To establish a role for lysosomes in APP metabolism in CHO

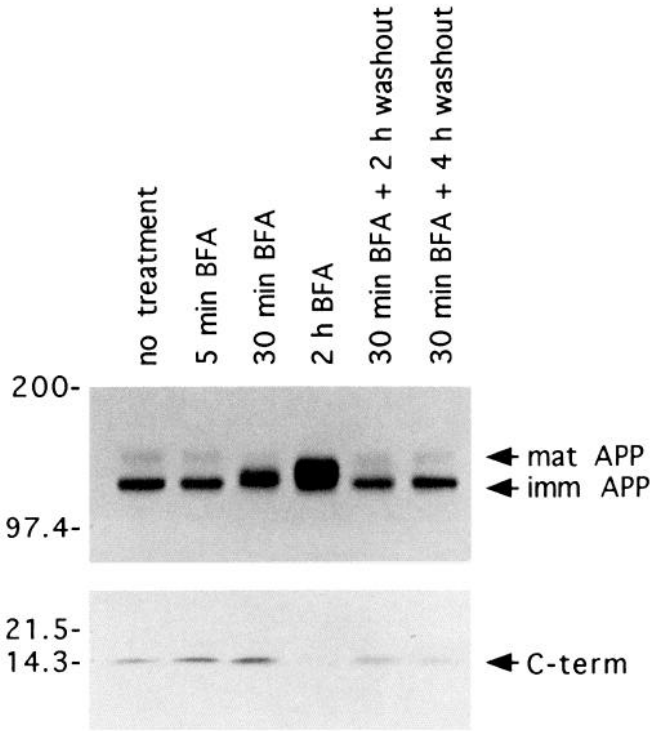

Figure 9. Immunoblot analysis of CHO cells treated with BFA. CHO cells were untreated or incubated with 10 μg/ml BFA for 5 min, 30 min, or 2 hr, or for 30 min followed by incubation in the absence of BFA for 2 or 4 hr, then lysed with 1% SDS. Proteins (50 μg) were separated on a 4–15% SDS-polyacrylamide gel, transferred to nitrocellulose, and probed with antibody 369A. The major APP-immunoreactive protein band of approximately 128 kDa seen at 0 min represents immature full-length APP. Mature full-length APP appears as a faint band at approximately 145 kDa. The protein band of approximately 14 kDa represents the carboxyl-terminal fragment resulting from APP secretory cleavage. Two hour BFA treatment results in abnormal APP posttranslational processing and inhibits APP secretory processing as demonstrated by the virtual absence of the 14 kDa fragment. Relative molecular masses in kilodaltons are indicated.

cells, cells were double labeled for APP and lgp120, an integral membrane protein of lysosomes (Lewis et al., 1985). In untreated cells, lgp120 immunostaining was punctate and dispersed throughout the cytoplasm, but was most prevalent at a juxtanuclear location that coincided with the region enriched in APP (Fig. 13*a'*). However, within this region the lgp120-positive puncta were clearly different from the more diffuse APP immunoreactivity. The lgp120-positive puncta have been shown to represent individual lysosomes (Lewis et al., 1985). There was little or no colocalization of APP immunoreactivity and the punctate lgp120 immunoreactivity in untreated cells (Fig. 13*a,a'*).

Following a 4 hr incubation in the presence of the weakly basic lysosomotropic agent chloroquine (de Duve et al., 1974), lgp120 immunoreactivity was no longer dispersed throughout the cytoplasm, but consisted of scattered clumps of punctate staining (Fig. 13*b'*). This is consistent with the lysosomal swelling seen in cells treated with weak bases (Ohkuma and Poole, 1981). APP immunostaining in the Golgi region was still present (Fig. 13*b*). However, there was striking colocalization of APP and lgp120 staining. Immunoblot analysis revealed an accumulation of mature APP and the 14 kDa carboxyl-terminal APP fragment, but no change in immature APP levels, in cells treated with chloroquine (Fig. 14).

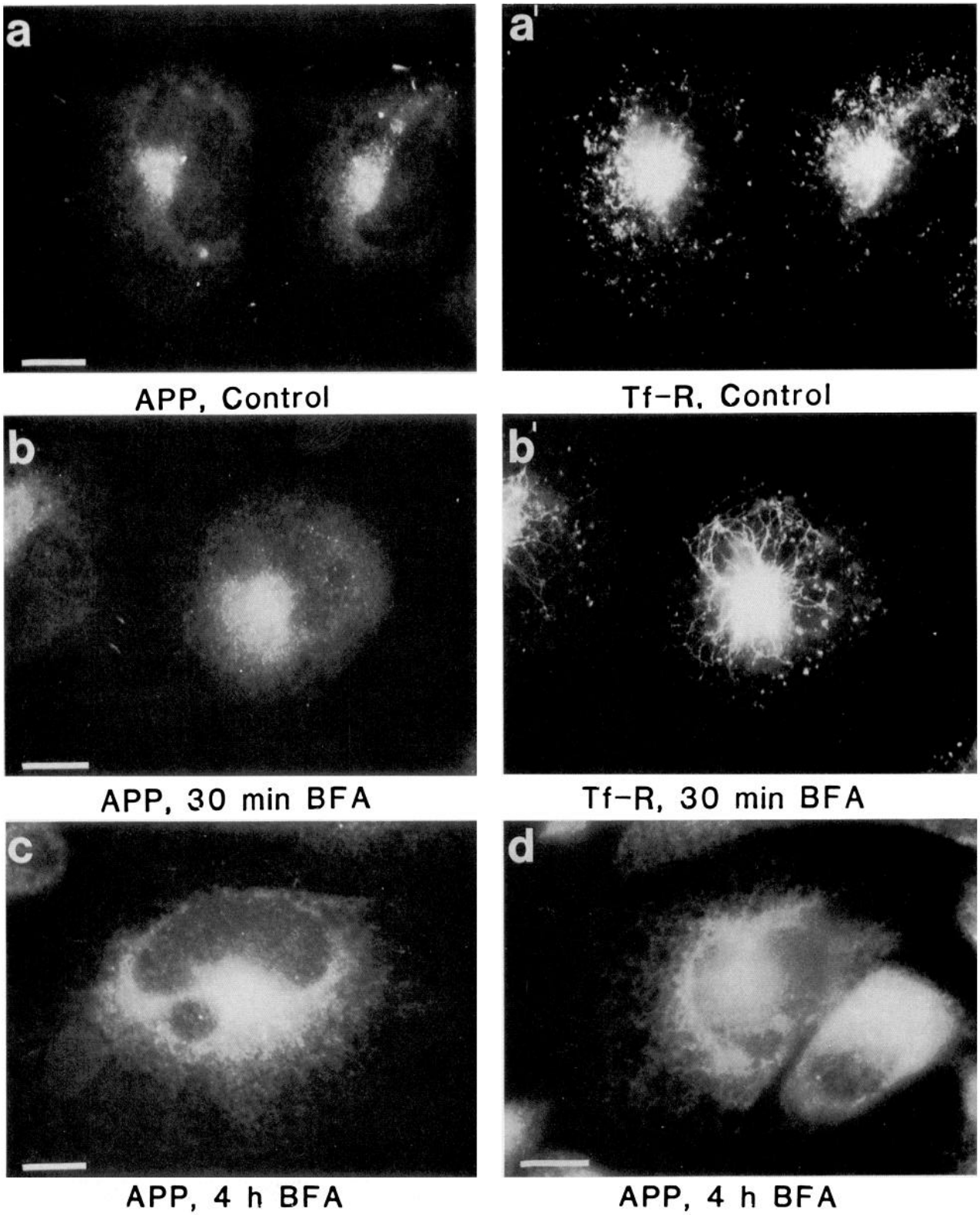

Figure 10. Comparison of the distributions of APP and Tf-R by immunofluorescence microscopy in control CHO cells and in CHO cells treated with BFA. Cells were untreated (*a, a'*) or treated with 10 μg/ml BFA for 30 min (*b, b'*) or 4 hr (*c, d*), fixed, and double labeled for APP (antibody 369A; *a, b*) and Tf-R (*a', b'*), or labeled for APP alone (*c, d*). Scale bars, 10 μm.

→

Figure 11. Comparison of the distributions of APP, Tf-R, and BiP by immunofluorescence microscopy in control COS cells and in COS cells treated with BFA. Cells were untreated (*a, a', c, c'*) or treated with 10 μg/ml BFA for 30 min (*b, b', d, d'*), washed, fixed, and double labeled for APP (antibody 369A; *a–d*) and Tf-R (*a', b'*) or BiP (*c', d'*). Scale bars, 10 μm.

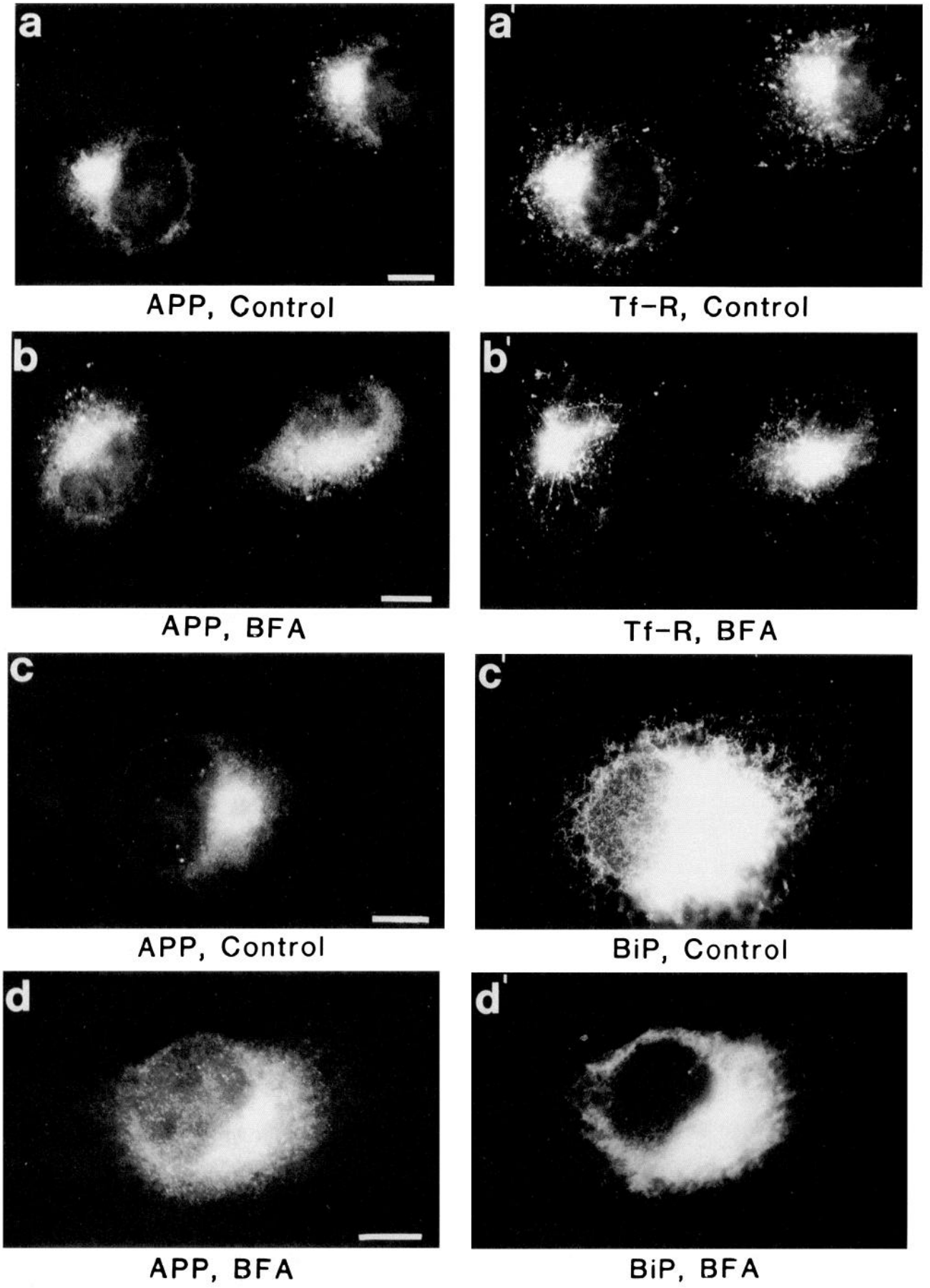
a
a'
APP, Control
Tf-R, Control
b
b'
APP, BFA
Tf-R, BFA
c
c'
APP, Control
BiP, Control
d
d'
APP, BFA
BiP, BFA

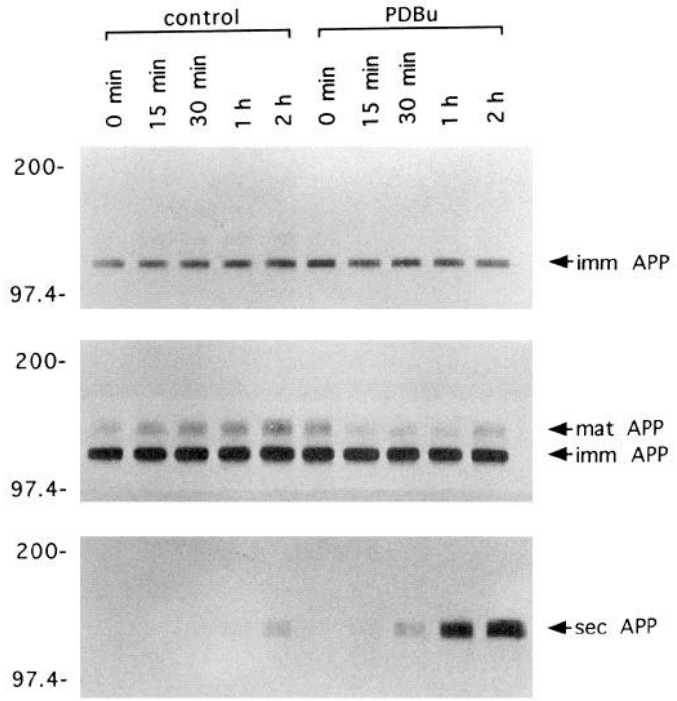

Figure 12. Immunoblot analysis of CHO cells treated with phorbol ester. Cells were incubated with medium alone or with medium containing 1 μM PDBu for the indicated times. Proteins from cell lysates (50 μg) or culture medium were separated on 7.5% SDS-polyacrylamide gels, transferred to nitrocellulose, and probed with antibody 22C11. Full-length immature and mature APP appear in cell lysates as 128 and 145 kDa proteins, respectively (*top* and *middle*), and secreted APP appears in conditioned medium as a 134 kDa protein (*bottom*). The *top and middle panels* represent different length exposures of the same immunoblot to optimize signal clarity for immature and mature APP, respectively. Relative molecular masses in kilodaltons are indicated.

Discussion

Much has been learned about the cell biology of APP since the cloning of its gene and elucidation of its structure (Kang et al., 1987). Nevertheless, investigative efforts have not yet yielded a comprehensive scheme for the cellular trafficking and metabolic pathways of this molecule. In this study, we have investigated the cellular trafficking of APP by examining the relationship between the subcellular localization of APP and its biochemical processing.

A striking feature of the distribution of APP within the cell is its high concentration in the region of the Golgi complex. In rat brain, in primary cultures of rat hippocampal neurons, and in cultures of several non-neuronal mammalian cell lines, APP immunoreactivity was localized to the region of the Golgi complex as demonstrated by several Golgi markers. A concentration of APP in the Golgi complex is in agreement with the perinuclear distribution for APP reported previously (Card et al., 1988; Martin et al., 1991; Schubert et al., 1991; Haass et al., 1992a). In those earlier studies, however, the precise localization of APP in the perinuclear area was not investigated.

The predominant localization of immunoreactivity in the Golgi complex is not in contrast with the predominant presence of immature APP in most cells as suggested by immunoblot analysis. Light microscopy immunocytochemistry revealed primarily sites of high antigen concentration in the region of the Golgi complex, whereas the large pool of APP in the ER appears simply as diffuse fluorescence.

Our data are consistent with a model in which APP is concentrated in the *trans*-Golgi and TGN during its transit through the central vacuolar system (Palade, 1975). Unfortunately, the presence of APP at the TGN could not be assessed by immunoelectron microscopy, because the experimental procedure resulted in the disruption of the TGN. Other experimental protocols (i.e., ultrathin frozen sectioning) did not allow sufficient labeling of APP with the antibodies used.

Concentration of the protein as it moves through the most distal Golgi compartments would occur prior to its dispersal in carrier vesicles to the cell surface or endocytic compartment (Griffiths and Simons, 1986). In addition to the intense Golgi staining, there was visible throughout the cell diffuse punctate APP immunoreactivity, which most likely represents these carrier vesicles. Concentration of immunoreactivity in the *trans* regions of the Golgi complex can be observed for proteins that travel through the secretory pathway and that are destined for secretion in the plasma membrane (Farquhar, 1985; Griffiths and Simons, 1986). Thus, this localization is in agreement with what is known about the biochemical processing of APP.

Our results with BFA argue against the possibility that accumulation of APP in the distal Golgi complex reflects a recycling of mature APP, or of its carboxyl-terminal fragment, between the TGN and early endosomes. Although BFA induced the formation of a reticulum between the TGN and endosomal system—as identified by Tf-R, a marker for early endosomes (Stoorvogel et al., 1988; Cameron et al., 1991)—no APP immunoreactivity was present in this structure. BFA treatment also resulted in accumulation of full-length APP and inhibition of APP secretion. These results are in agreement with inhibition by BFA of the transport to the plasma membrane and secretion of several proteins (Takatsuki and Tamura, 1985; Misumi et al., 1986; Fujiwara et al., 1988; Magner and Papagiannes, 1988), as well as with the relocation without functional impairment of Golgi enzymes to the ER (Doms et al., 1989). Since BFA has been shown to dissect functionally the *trans*-Golgi from the TGN (Chege and Pfeffer, 1990), our results indicate that APP secretory cleavage occurs distal to the *trans*-Golgi.

It seems unlikely that APP is a resident Golgi protein. In contrast to some resident Golgi proteins such as mannosidase II or galactosyltransferase, which have half-lives of about 20 hr (Strous and Berger, 1982; Moreman and Touster, 1985), APP was shown by pulse-chase analysis in PC12 cells to turn over with a half-life of less than 2 hr (Weidemann et al., 1989; Caporaso et al., 1992a). In addition, there is strong evidence for trafficking of APP to compartments distal to the Golgi complex (i.e., the plasma membrane and lysosomes) (Haass et al., 1992a; Sisodia, 1992).

The precise mechanism by which phorbol esters affect APP proteolytic processing is not yet understood. Activation of protein kinase C by phorbol esters stimulates the turnover of mature full-length APP in PC12 cells (Buxbaum et al., 1990) and increases APP secretion (Caporaso et al., 1992b). Mature full-length APP and carboxyl-terminal APP fragments have been shown to be substrates for protein kinase C (Gandy et al., 1988; Suzuki et al., 1992), but the significance, if any, of APP phosphorylation on its processing remains to be determined. Alternatively, PDBu might exert its effect on a component of the APP processing apparatus. In an attempt to assess whether phorbol esters exert their effect on APP processing by altering the

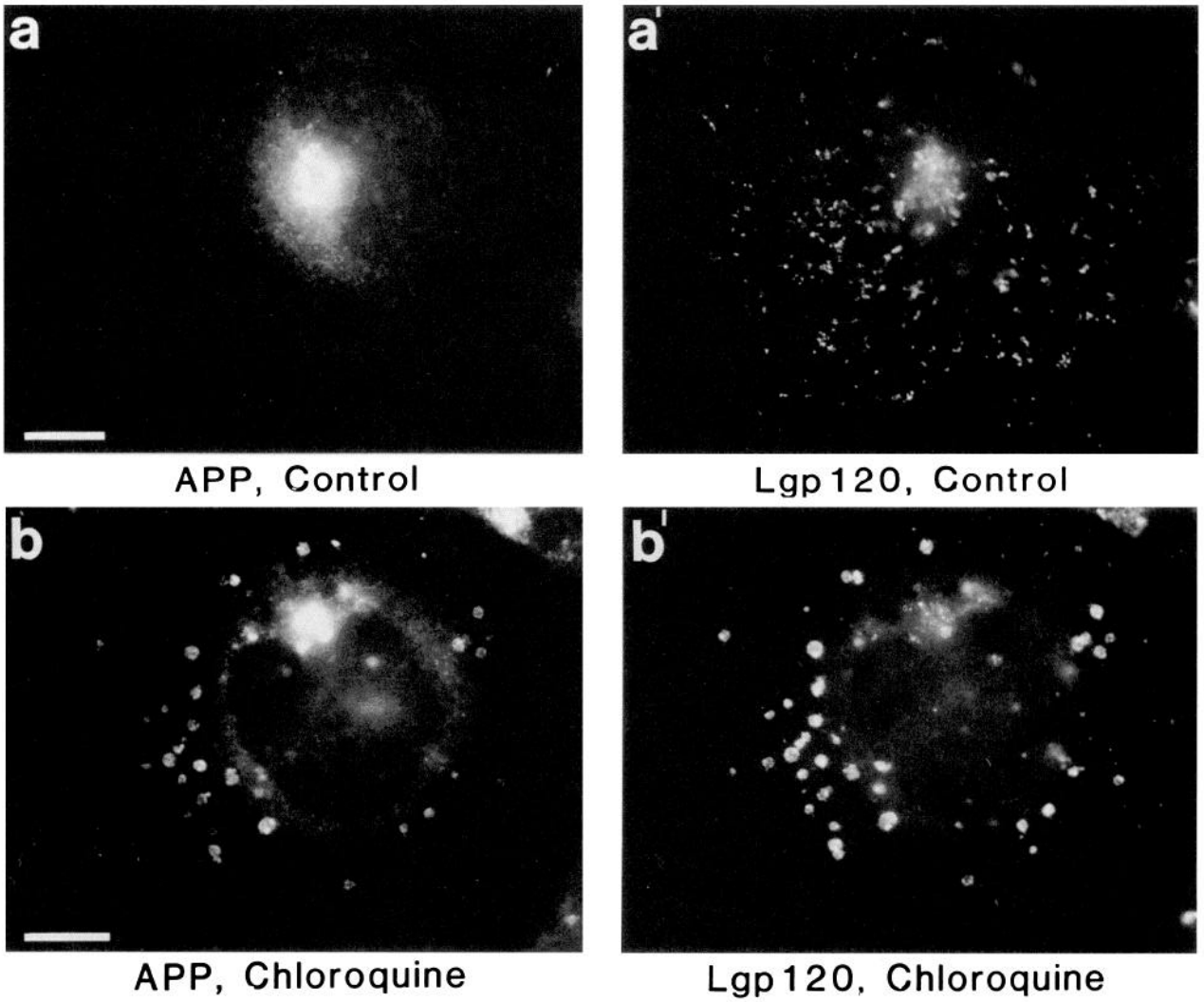

Figure 13. Comparison of the distributions of APP and lgp120 by immunofluorescence microscopy in control CHO cells and in CHO cells treated with chloroquine. Cells were untreated (*a, a'*) or treated with 50 μM chloroquine for 4 hr (*b, b'*), fixed, and double labeled for APP (antibody 369A; *a, b*) and lgp120 (*a', b'*). Scale bars, 10 μm.

movement of APP molecules, we examined whether APP cellular immunoreactivity could be redistributed by treatment of cells with PDBu. No apparent change in APP immunolocalization was observed when using different carboxyl-terminal APP antibodies.

The present study provides strong evidence that APP is targeted to lysosomes for proteolytic processing. In cells treated with the weak base chloroquine (de Duve et al., 1974), there was extensive colocalization of APP and the lysosomal integral membrane protein lgp120 (Lewis et al., 1985), though little or no colocalization was seen in untreated cells (Fig. 13). There was no accumulation of APP immunoreactivity in the region of the Golgi complex, indicating that the effects of chloroquine on APP processing do not occur at the TGN, which is an acidic cellular compartment that might be sensitive to weak bases (Anderson and Pathak, 1985). Also, the results suggest that APP is rapidly proteolyzed in lysosomes, since APP could be seen in these structures only when lysosomal proteolysis was inhibited by chloroquine. This was apparent by the accumulation, in lysates from chloroquine-treated cells, of mature full-length APP and the carboxyl-terminal APP fragment resulting from secretory cleavage (Fig. 14). These results agree with other studies indicating that lysosomotropic agents can affect APP proteolytic processing (Cole et al., 1989; Caporaso et al., 1992a; Golde et al., 1992; Knops et al., 1992) or cause accumulation of APP and APP degradation products in vesicular structures identified as lysosomes (Haass et al., 1992a). The conclusion that lysosomes play a role in the pathogenesis of Alzheimer disease, however, would require definitive evidence that lysosome-specific enzymes can produce β/A4 amyloid peptide *in vitro* or in cell-free preparations. The recent demonstration that lysosomotropic agents can alter the production of β/A4 peptide from cultured cells (Shoji et al., 1992) should facilitate the study of the precise cellular locus for the production of β/A4 amyloid.

An intriguing finding from this study was the immunoelectron microscopic localization of APP to medium-sized, apparently invaginated vesicles in axons and dendrites (Fig. 3). The punctate APP staining seen in the proximal segments of axons (Fig. 1) and in the processes of hippocampal neurons (Fig. 2) might at least be partially accounted for by these vesicles. These structures may be carrier vesicles for APP, though it remains to be established whether they are migrating from the Golgi complex

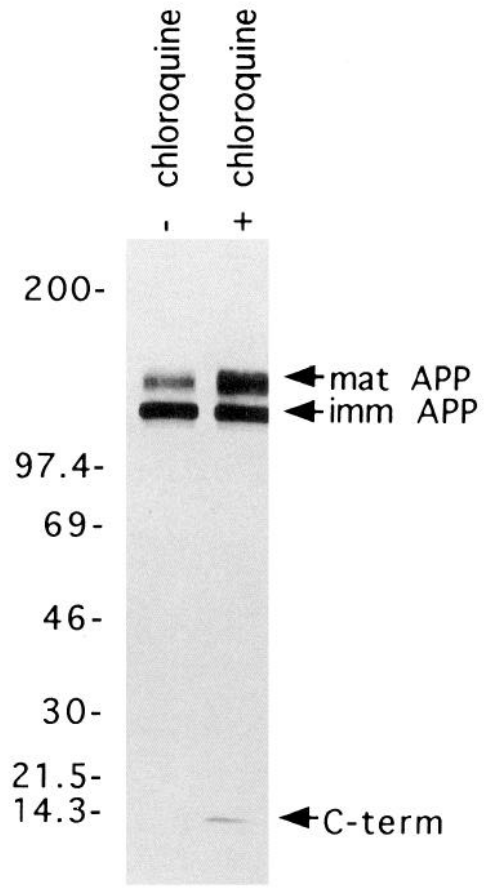

Figure 14. Immunoblot analysis of CHO cells treated with chloroquine. Cells were incubated with medium alone or with medium containing 50 μM chloroquine for 4 hr. Proteins from cell lysates (50 μg) were separated on a 4–15% SDS-polyacrylamide gel, transferred to nitrocellulose, and probed with antibody 369A. Full-length immature and mature APP appear as 128 and 145 kDa proteins, respectively, and the carboxyl-terminal APP fragment resulting from secretory cleavage appears as an approximately 14 kDa protein. Relative molecular masses in kilodaltons are indicated.

to the cell periphery or vice versa or both. Studies with ligated rat sciatic nerve revealed that APP undergoes anterograde fast axonal transport, but the organelles responsible for this transport were not identified (Koo et al., 1990). Structures ("compound double vesicles") similar to the ones observed in the present report have been seen in the cell body and axon of the giant cerebral neuron of *Aplysia*, and have been suggested to be vesicles on their way to nerve terminals (Shkolnik and Schwartz, 1980). Schubert et al. (1991) reported an association of APP with presynaptic vesicles. Our data argue against the presence of significant amounts of APP in synaptic vesicles and do not indicate a concentration of APP at CNS synapses (Fig. 3).

On the other hand, the APP-positive vesicles may mediate retrograde transport of APP or its carboxyl-terminal fragment. The inner membranes of these structures appear to arise by invagination of the outer membranes and therefore bear similarity to multivesicular bodies (late endosomes), which are known to be involved in retrograde axonal flow (Tsukita and Ishikawa, 1980; Parton et al., 1992). In addition, trafficking through multivesicular bodies could provide a means by which APP is targeted to lysosomes and by which it is released from the membrane so that proteolytic processing to β/A4 peptide could occur (Gandy et al., 1992). Further study is required to clarify the role of these structures in APP trafficking.

References

Anderson RGW, Pathak RK (1985) Vesicles and cisternae in the *trans* Golgi apparatus of human fibroblasts are acidic compartments. Cell 40:635–643.

Banker GA, Cowan WM (1977) Rat hippocampal neurons in dispersed cell culture. Brain Res 126:397–425.

Bartlett WP, Banker GA (1984) An electron microscopic study of the development of axons and dendrites by hippocampal neurons in culture. I. Cells which develop without intercellular contacts. J Neurosci 4:1944–1953.

Benowitz LI, Rodriguez W, Paskevich P, Mufson EJ, Schenk D, Neve RL (1989) The amyloid precursor protein is concentrated in neuronal lysosomes in normal and Alzheimer disease subjects. Exp Neurol 106:237–250.

Bole DG, Hendershot LM, Kearney JF (1986) Posttranslational association of immunoglobulin heavy chain binding protein with nascent heavy chains in nonsecreting and secreting hybridomas. J Cell Biol 102:1558–1566.

Buckley K, Kelly RB (1985) Identification of a transmembrane glycoprotein specific for secretory vesicles of neural and endocrine cells. J Cell Biol 100:1284–1294.

Buxbaum JD, Gandy SE, Cicchetti P, Ehrlich ME, Czernik AJ, Fracasso RP, Ramabhadran TV, Unterbeck AJ, Greengard P (1990) Processing of Alzheimer β/A4 amyloid precursor protein: modulation by agents that regulate protein phosphorylation. Proc Natl Acad Sci USA 87:6003–6006.

Buxbaum JD, Oishi M, Chen HI, Pinkas-Kramarski R, Jaffe EA, Gandy SE, Greengard P (1992) Cholinergic agonists and interleukin 1 regulate processing and secretion of the Alzheimer β/A4 amyloid protein precursor. Proc Natl Acad Sci USA 89:10075–10078.

Cameron PL, Südhof TC, Jahn R, De Camilli P (1991) Colocalization of synaptophysin with transferrin receptors: implications for synaptic vesicle biogenesis. J Cell Biol 115:151–164.

Caporaso GL, Gandy SE, Buxbaum JD, Greengard P (1992a) Chloroquine inhibits intracellular degradation but not secretion of Alzheimer β/A4 amyloid precursor protein. Proc Natl Acad Sci USA 89: 2252–2256.

Caporaso GL, Gandy SE, Buxbaum JD, Ramabhadran TV, Greengard P (1992b) Protein phosphorylation regulates secretion of Alzheimer β/A4 amyloid precursor protein. Proc Natl Acad Sci USA 89:3055–3059.

Card JP, Meade RP, Davis LG (1988) Immunocytochemical localization of the precursor protein for β-amyloid in the rat central nervous system. Neuron 1:835–846.

Chartier-Harlin M-C, Crawford F, Houlden H, Warren A, Hughes D, Fidani L, Goate A, Rossor M, Roques P, Hardy J, Mullan M (1991) Early-onset Alzheimer's disease caused by mutations at codon 717 of the β-amyloid precursor protein gene. Nature 353:844–846.

Chege NW, Pfeffer SR (1990) Compartmentation of the Golgi complex: brefeldin-A distinguishes *trans*-Golgi cisternae from the *trans*-Golgi network. J Cell Biol 111:893–899.

Cole GM, Huynh TV, Saitoh T (1989) Evidence for lysosomal processing of amyloid β-protein precursor in cultured cells. Neurochem Res 14:933–939.

De Camilli P, Cameron R, Greengard P (1983a) Synapsin I (protein I), a nerve terminal–specific phosphoprotein. I. Its general distribution in synapses of the central and peripheral nervous system demonstrated by immunofluorescence in frozen and plastic sections. J Cell Biol 96:1337–1354.

De Camilli P, Harris SM Jr, Huttner WB, Greengard P (1983b) Synapsin I (protein I), a nerve terminal–specific phosphoprotein. II. Its specific association with synaptic vesicles demonstrated by immunocytochemistry in agarose-embedded synaptosomes. J Cell Biol 96: 1355–1373.

De Camilli P, Moretti M, Denis Donini S, Walter U, Lohmann SM (1986) Heterogeneous distribution of the cAMP receptor protein RII in the nervous system: evidence for its intracellular accumulation on microtubules, microtubule-organizing centers, and in the area of the Golgi complex. J Cell Biol 103:189–203.

de Duve C, de Barsy T, Poole B, Trouet A, Tulkens P, Van Hoof F (1974) Commentary. Lysosomotropic drugs. Biochem Pharmacol 23:2495–2531.

Doms RW, Russ G, Yewdell JW (1989) Brefeldin A redistributes resident and itinerant Golgi proteins to the endoplasmic reticulum. J Cell Biol 109:61–72.

Efrat S, Linde S, Kofod H, Spector D, Delannoy M, Grant S, Hanahan D, Baekkeskov S (1988) Beta-cell lines derived from transgenic mice expressing a hybrid insulin gene-oncogene. Proc Natl Acad Sci USA 85:9037–9041.

Esch FS, Keim PS, Beattie EC, Blacher RW, Culwell AR, Oltersdorf T, McClure D, Ward PJ (1990) Cleavage of amyloid β peptide during constitutive processing of its precursor. Science 248:1122–1124.

Farquhar MG (1985) Progress in unraveling pathways of Golgi traffic. Annu Rev Cell Biol 1:447–488.

Fujiwara T, Oda K, Yokota S, Takatsuki A, Ikehara Y (1988) Brefeldin A causes disassembly of the Golgi complex and accumulation of secretory proteins in the endoplasmic reticulum. J Biol Chem 263: 18545–18552.

Gandy S, Czernik AJ, Greengard P (1988) Phosphorylation of Alzheimer disease amyloid precursor peptide by protein kinase C and Ca^{2+}/calmodulin-dependent protein kinase II. Proc Natl Acad Sci USA 85:6218–6221.

Gandy SE, Buxbaum JD, Greengard P (1992) A cell biological approach to the therapy of Alzheimer-type cerebral β/A4-amyloidosis. In: Alzheimer's disease. New treatment strategies (Khachaturian ZS, Blass JP, eds), pp 175–192. New York: Dekker.

Gazdar AF, Chick WL, Oie HK, Sims HL, King DL, Weir GC, Lauris V (1980) Continuous, clonal, insulin- and somatostatin-secreting cell lines established from a transplantable rat islet cell tumor. Proc Natl Acad Sci USA 77:3519–3523.

Gillespie SL, Golde TE, Younkin SG (1992) Secretory processing of the Alzheimer amyloid β/A4 protein precursor is increased by protein phosphorylation. Biochem Biophys Res Commun 187:1285–1290.

Glenner GG, Wong CW (1984) Alzheimer's disease: initial report of the purification and characteristics of a novel cerebrovascular amyloid protein. Biochem Biophys Res Commun 120:885–890.

Goate A, Chartier-Harlin M-C, Mullan M, Brown J, Crawford F, Fidani L, Giuffra L, Haynes A, Irving N, James L, Mant R, Newton P, Rooke K, Roques P, Talbot C, Pericak-Vance M, Roses A, Williamson R, Rossor M, Owen M, Hardy J (1991) Segregation of a missense mutation in the amyloid precursor protein gene with familial Alzheimer's disease. Nature 349:704–706.

Golde TE, Estus S, Younkin LH, Selkoe DJ, Younkin SG (1992) Processing of the amyloid protein precursor to potentially amyloidogenic derivatives. Science 255:728–730.

Goldgaber D, Lerman MI, McBride OW, Saffiotti U, Gajdusek DC (1987) Characterization and chromosomal localization of a cDNA encoding brain amyloid of Alzheimer's disease. Science 235:877–880.

Goldgaber D, Harris HW, Hla T, Maciag T, Donnelly RJ, Jacobsen JS, Vitek MP, Gajdusek DC (1989) Interleukin 1 regulates synthesis of amyloid β-protein precursor mRNA in human endothelial cells. Proc Natl Acad Sci USA 86:7606–7610.

Griffiths G, Simons K (1986) The *trans* Golgi network: sorting at the exit site of the Golgi complex. Science 234:438–443.

Haass C, Hung AY, Selkoe DJ (1991) Processing of β-amyloid precursor protein in microglia and astrocytes favors an internal localization over constitutive secretion. J Neurosci 11:3783–3793.

Haass C, Koo EH, Mellon A, Hung AY, Selkoe DJ (1992a) Targeting of cell-surface β-amyloid precursor protein to lysosomes: alternative processing into amyloid-bearing fragments. Nature 357:500–503.

Haass C, Schlossmacher MG, Hung AY, Vigo-Pelfrey C, Mellon A, Ostaszewski BL, Lieberburg I, Koo EH, Schenk D, Teplow DB, Selkoe DJ (1992b) Amyloid β-peptide is produced by cultured cells during normal metabolism. Nature 359:322–325.

Hendriks L, van Duijn CM, Cras P, Cruts M, Van Hul W, van Harskamp F, Warren A, McInnis MG, Antonarakis SE, Martin J-J, Hofman A, Van Broeckhoven C (1992) Presenile dementia and cerebral haemorrhage linked to a mutation at codon 692 of the β-amyloid precursor protein gene. Nature Genet 1:218–221.

Kang J, Lemaire H-G, Unterbeck A, Salbaum JM, Masters CL, Grzeschik K-H, Multhaup G, Beyreuther K, Müller-Hill B (1987) The precursor of Alzheimer's disease amyloid A4 protein resembles a cell-surface receptor. Nature 325:733–736.

Kitaguchi N, Takahashi Y, Tokushima Y, Shiojiri S, Ito H (1988) Novel precursor of Alzheimer's disease amyloid protein shows protease inhibitory activity. Nature 331:530–532.

Klausner RD, Donaldson JG, Lippincott-Schwartz J (1992) Brefeldin A: insights into the control of membrane traffic and organelle structure. J Cell Biol 116:1071–1080.

Knops J, Lieberburg I, Sinha S (1992) Evidence for a nonsecretory, acidic degradation pathway for amyloid precursor protein in 293 cells. Identification of a novel, 22-kDa, β-peptide–containing intermediate. J Biol Chem 267:16022–16024.

Koo EH, Sisodia SS, Archer DR, Martin LJ, Weidemann A, Beyreuther K, Fischer P, Masters CL, Price DL (1990) Precursor of amyloid protein in Alzheimer disease undergoes fast anterograde axonal transport. Proc Natl Acad Sci USA 87:1561–1565.

Laemmli UK (1970) Cleavage of structural proteins during the assembly of the head of bacteriophage T4. Nature 227:680–685.

Levy E, Carmen MD, Fernandez-Madrid IJ, Power MD, Lieberburg I, van Duinen SG, Bots GThAM, Luyendijk W, Frangione B (1990) Mutation of the Alzheimer's disease amyloid gene in hereditary cerebral hemorrhage, Dutch type. Science 248:1124–1126.

Lewis V, Green SA, Marsh M, Vihko P, Helenius A, Mellman I (1985) Glycoproteins of the lysosomal membrane. J Cell Biol 100:1839–1847.

Lippincott-Schwartz J, Yuan LC, Bonifacino JS, Klausner RD (1989) Rapid redistribution of Golgi proteins into the ER in cells treated with brefeldin A: evidence for membrane cycling from Golgi to ER. Cell 56:801–813.

Lippincott-Schwartz J, Yuan L, Tipper C, Amherdt M, Orci L, Klausner RD (1991) Brefeldin A's effects on endosomes, lysosomes, and the TGN suggest a general mechanism for regulating organelle structure and membrane traffic. Cell 67:601–616.

Magner JA, Papagiannes E (1988) Blockade by brefeldin A of intracellular transport of secretory proteins in mouse pituitary cells: effects on the biosynthesis of thyrotropin and free α-subunits. Endocrinology 122:912–920.

Martin LJ, Sisodia SS, Koo EH, Cork LC, Dellovade TL, Weidemann A, Beyreuther K, Masters C, Price DL (1991) Amyloid precursor protein in aged nonhuman primates. Proc Natl Acad Sci USA 88: 1461–1465.

Masters CL, Simms G, Weinman NA, Multhaup G, McDonald BL, Beyreuther K (1985) Amyloid plaque protein in Alzheimer disease and Down syndrome. Proc Natl Acad Sci USA 82:4245–4249.

Misumi Y, Misumi Y, Miki K, Takatsuki A, Tamura G, Ikehara Y (1986) Novel blockade by brefeldin A of intracellular transport of secretory proteins in cultured rat hepatocytes. J Biol Chem 261:11398–11403.

Moreman KW, Touster O (1985) Biosynthesis and modification of Golgi mannosidase II in HeLa and 3T3 cells. J Biol Chem 260:6654–6662.

Mullan M, Crawford F, Axelman K, Houlden H, Lilius L, Winblad B, Lannfelt L (1992) A pathogenic mutation for probable Alzheimer's disease in the APP gene at the N-terminus of β-amyloid. Nature Genet 1:345–347.

Murrell J, Farlow M, Ghetti B, Benson MD (1991) A mutation in the amyloid precursor protein associated with hereditary Alzheimer's disease. Science 254:97–99.

Naruse S, Igarashi S, Kobayashi H, Aoki K, Inuzuka T, Kaneko K, Simizu T, Iihara K, Kojima T, Miyatake T, Tsuji S (1991) Missense mutation Val-to-Ile in exon 17 of amyloid precursor protein gene in Japanese familial Alzheimer's disease. Lancet 337:978–979.

Nitsch RM, Slack BE, Wurtman RJ, Growdon JH (1992) Release of Alzheimer amyloid precursor derivatives stimulated by activation of muscarinic acetylcholine receptors. Science 258:304–307.

Nordstedt C, Caporaso GL, Thyberg J, Gandy SE, Greengard P (1993) Identification of the Alzheimer β/A4 amyloid precursor protein in clathrin-coated vesicles purified from PC12 cells. J Biol Chem 268: 608–612.

Novikoff PM, Tulsiani DRP, Touster O, Yam A, Novikoff AB (1983) Immunocytochemical localization of α-D-mannosidase II in the Golgi apparatus of rat liver. Proc Natl Acad Sci USA 80:4364–4368.

Ohkuma S, Poole B (1981) Cytoplasmic vacuolation of mouse peritoneal macrophages and the uptake into lysosomes of weakly basic substances. J Cell Biol 90:656–664.

Oltersdorf T, Ward PJ, Henriksson T, Beattie EC, Neve R, Lieberburg I, Fritz LC (1990) The Alzheimer amyloid precursor protein. Identification of a stable intermediate in the biosynthetic/degradative pathway. J Biol Chem 265:4492–4497.

Overly CC, Fritz LC, Lieberburg I, McConlogue L (1991) The β-amyloid precursor protein is not processed by the regulated secretory pathway. Biochem Biophys Res Commun 181:513–519.

Palade G (1975) Intracellular aspects of the process of protein synthesis. Science 189:347–358.

Palmert MR, Berman Podlisny M, Witker DS, Oltersdorf T, Younkin LH, Selkoe DJ, Younkin SG (1989) The β-amyloid protein precursor of Alzheimer disease has soluble derivatives found in human brain and cerebrospinal fluid. Proc Natl Acad Sci USA 86:6338–6342.

Parton RG, Simons K, Dotti CG (1992) Axonal and dendritic endocytic pathways in cultured neurons. J Cell Biol 119:123–137.

Pelham HRB (1991) Multiple targets for brefeldin A. Cell 67:449–451.

Podlisny MB, Tolan DR, Selkoe DJ (1991) Homology of the amyloid beta protein precursor in monkey and human supports a primate model for beta amyloidosis in Alzheimer's disease. Am J Pathol 138: 1423–1435.

Ponte P, Gonzalez-DeWhitt P, Schilling J, Miller J, Hsu D, Greenberg B, Davis K, Wallace W, Lieberburg I, Fuller F, Cordell B (1988) A new A4 amyloid mRNA contains a domain homologous to serine proteinase inhibitors. Nature 331:525–527.

Reaves B, Banting G (1992) Perturbation of the morphology of the *trans*-Golgi network following brefeldin A treatment: redistribution of a TGN-specific integral membrane protein, TGN38. J Cell Biol 116:85–94.

Ridgway ND, Dawson PA, Ho YK, Brown MS, Goldstein JL (1992) Translocation of oxysterol binding protein to Golgi apparatus triggered by ligand binding. J Cell Biol 116:307–319.

Robakis NK, Ramakrishna N, Wolfe G, Wisniewski HM (1987) Molecular cloning and characterizations of a cDNA encoding the cerebrovascular and the neuritic plaque amyloid peptides. Proc Natl Acad Sci USA 84:4190–4194.

Saraste J, Palade GE, Farquhar MG (1987) Antibodies to rat pancreas Golgi subfractions: identification of a 58-kD *cis*-Golgi protein. J Cell Biol 105:2021–2029.

Schubert W, Prior R, Weidemann A, Dircksen H, Multhaup G, Masters CL, Beyreuther K (1991) Localization of Alzheimer βA4 amyloid precursor protein at central and peripheral synaptic sites. Brain Res 563:184–194.

Seubert P, Vigo-Pelfrey C, Esch F, Lee M, Dovey H, Davis D, Sinha S, Schlossmacher M, Whaley J, Swindlehurst C, McCormack R, Wolfert R, Selkoe D, Lieberburg I, Schenk D (1992) Isolation and quantification of soluble Alzheimer's β-peptide from biological fluids. Nature 359:325–327.

Shkolnik LJ, Schwartz JH (1980) Genesis and maturation of serotonergic vesicles in identified giant cerebral neuron of *Aplysia*. J Neurophysiol 43:945–967.

Shoji M, Golde TE, Ghiso J, Cheung TT, Estus S, Shaffer LM, Cai X-D, McKay DM, Tintner R, Frangione B, Younkin SG (1992) Production of the Alzheimer amyloid β protein by normal proteolytic processing. Science 258:126–129.

Sisodia SS (1992) β-amyloid precursor protein cleavage by a membrane-bound protease. Proc Natl Acad Sci USA 89:6075–6079.

Sisodia SS, Koo EH, Beyreuther K, Unterbeck A, Price DL (1990) Evidence that β-amyloid protein in Alzheimer's disease is not derived by normal processing. Science 248:492–495.

Slot JW, Geuze HJ (1985) A new method of preparing gold probes for multiple-labeling cytochemistry. Eur J Cell Biol 38:87–93.

Stoorvogel W, Geuze HJ, Griffith JM, Strous GJ (1988) The pathways of endocytosed transferrin and secretory protein are connected in the *trans*-Golgi reticulum. J Cell Biol 106:1821–1829.

Strous GJAM, Berger EG (1982) Biosynthesis, intracellular transport, and release of the Golgi enzyme galactosyltransferase (lactose synthetase A protein) in HeLa cells. J Biol Chem 257:7623–7628.

Suzuki T, Nairn AC, Gandy SE, Greengard P (1992) Phosphorylation of Alzheimer amyloid precursor protein by protein kinase C. Neuroscience 48:755–761.

Takatsuki A, Tamura G (1985) Brefeldin A, a specific inhibitor of intracellular translocation of vesicular stomatitis virus G protein: intracellular accumulation of high-mannose type G protein and inhibition of its cell surface expression. Agric Biol Chem 49:899–902.

Takei K, Stukenbrok H, Metcalf A, Mignery GA, Südhof TC, Volpe P, De Camilli P (1992) Ca^{2+} stores in Purkinje neurons: endoplasmic reticulum subcompartments demonstrated by the heterogeneous distribution of the InsP3 receptor, Ca^{2+}-ATPase, and calsequestrin. J Neurosci 12:489–505.

Tanzi RE, Gusella JF, Watkins PC, Bruns GAP, St George-Hyslop P, Van Keuren ML, Patterson D, Pagan S, Kurnit DM, Neve RL (1987) Amyloid β protein gene: cDNA, mRNA distribution, and genetic linkage near the Alzheimer locus. Science 235:880–884.

Tanzi RE, McClatchey AI, Lamperti ED, Villa-Komaroff L, Gusella JF, Neve RL (1988) Protease inhibitor domain encoded by an amyloid protein precursor mRNA associated with Alzheimer's disease. Nature 331:528–530.

Tartakoff AM, Vassalli P (1983) Lectin-binding sites as markers of Golgi subcompartments: proximal-to-distal maturation of oligosaccharides. J Cell Biol 97:1243–1248.

Teixidó J, Massagué J (1988) Structural properties of a soluble bioactive precursor for transforming growth factor-α. J Biol Chem 263: 3924–3929.

Tomlinson BE, Corsellis JAN (1984) Ageing and the dementias. In: Greenfield's neuropathology, 4th ed (Adams JH, Corsellis JAN, Duchen LW, eds), pp 951–1025. New York: Wiley.

Towbin H, Staehelin T, Gordon J (1979) Electrophoretic transfer of proteins from polyacrylamide gels to nitrocellulose sheets: procedure and some applications. Proc Natl Acad Sci USA 76:4350–4354.

Tsukita S, Ishikawa H (1980) The movement of membranous organelles in axons. Electron microscopic identification of anterogradely and retrogradely transported organelles. J Cell Biol 84:513–530.

Virtanen I, Ekblom P, Laurila P (1980) Subcellular compartmentalization of saccharide moieties in cultured normal and malignant cells. J Cell Biol 85:429–434.

Wasco W, Bupp K, Magendantz M, Gusella JF, Tanzi RE, Solomon F (1992) Identification of a mouse brain cDNA that encodes a protein related to the Alzheimer disease-associated amyloid β protein precursor. Proc Natl Acad Sci USA 89:10758–10762.

Wasco W, Gurubhagavatula S, Paradis Md, Romano DM, Sisodia SS, Hyman BT, Neve RL, Tanzi RE (1993) Isolation and characterization of *APLP2* encoding a homologue of the Alzheimer's associated amyloid β protein precursor. Nature Genet 5:95–100.

Weidemann A, König G, Bunke D, Fischer P, Salbaum JM, Masters CL, Beyreuther K (1989) Identification, biogenesis and localization of precursors of Alzheimer's disease A4 amyloid protein. Cell 57: 115–126.

Wood SA, Park JE, Brown WJ (1991) Brefeldin A causes a microtubule-mediated fusion of the *trans*-Golgi network and early endosomes. Cell 67:591–600.

Yuan L, Barriocanal JG, Bonifacino JS, Sandoval IV (1987) Two integral membrane proteins located in the *cis*-middle and *trans*-part of the Golgi system acquire sialylated N-linked carbohydrates and display different turnovers and sensitivity to cAMP-dependent phosphorylation. J Cell Biol 105:215–227.